Universality of phase transitions of frustrated antiferromagnets

1998 J. Phys.: Condens. Matter 10 4707

(http://iopscience.iop.org/0953-8984/10/22/004)

J. Phys.: Condens. Matter **10** (1998) 4707–4754. Printed in the UK PII: S0953-8984(98)91033-5

REVIEW ARTICLE

Universality of phase transitions of frustrated antiferromagnets

Hikaru Kawamura
Faculty of Engineering and Design, Kyoto Institute of Technology, Sakyo-ku, Kyoto 606, Japan

Received 26 January 1998

Abstract. Recent theoretical and experimental studies on the critical properties of frustrated antiferromagnets with non-collinear spin order, including stacked-triangular antiferromagnets and helimagnets, are reviewed. Particular emphasis is put on the novel critical and multicritical behaviours exhibited by these magnets, together with the important role played by the 'chirality'.

1. Introduction

Phase transitions and critical phenomena have been a central issue of statistical physics for many years. In particular, phase transitions of magnets or of 'spin systems' have attracted special interest. Thanks to extensive theoretical and experimental studies, we now have a rather good understanding of the nature of phase transitions of standard ferromagnets and antiferromagnets. By the term 'standard', I mean here regular and unfrustrated magnets without quenched disorder and frustration. They include ferromagnets and unfrustrated antiferromagnets with collinear spin order.

One key notion which emerged through these studies is the notion of universality. According to the universality hypothesis, a variety of continuous (or second-order) phase transitions can be classified into a small number of universality classes determined by a few basic properties characterizing the system under study, such as the space dimensionality d, the symmetry of the order parameter and the range of interaction. If one is interested only in the so-called universal quantities, such as critical exponents, amplitude ratios and scaled equations of state, various phase transitions should exhibit exactly the same behaviour. In the case of standard bulk magnets in three spatial dimensions ($d = 3$), the universality class is basically determined by the number of spin components, n. Physically, the index n is related to the type of magnetic anisotropy: that is, $n = 1$ (Ising), $n = 2$ (XY) and $n = 3$ (Heisenberg) correspond to magnets with easy-axis-type anisotropy, easy-plane-type anisotropy and no anisotropy (isotropic magnets), respectively. The critical properties associated with these n-component O(n) universality classes have been extensively studied and are now rather well understood. From the renormalization-group (RG) viewpoint, these critical properties are governed by the so-called Wilson–Fisher O(n) fixed point.

Of course, there are classes of magnets exhibiting phase transitions whose behaviours are very different from the standard O(n) behaviour. One example of such a class is the random magnets with quenched disorder. A typical example is a spin glass, a magnet not only random but also *frustrated*. Even in regular magnets without quenched disorder, one can expect novel transition behaviour if the magnets are frustrated. In fact, the nature of the phase transitions of frustrated magnets could be novel and entirely different from that of the phase transitions of conventional unfrustrated magnets, as we shall see in what follows.

0953-8984/98/224707+48$19.50

1.1. Frustration

Frustration could arise either from the special geometry of the lattice, or from the competition between the near-neighbour and further-neighbour interactions. The former type of frustration may be seen in antiferromagnets on a two-dimensional (2D) triangular lattice or on a three-dimensional (3D) stacked-triangular (simple hexagonal) lattice, which consists of two-dimensional triangular layers stacked along an orthogonal direction. The latter type of frustration may be realized in helimagnets where a magnetic spiral is formed along a certain direction of the lattice.

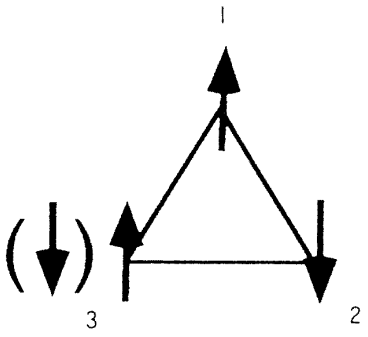

Figure 1. The ground-state spin configuration of three Ising spins on a triangle coupled antiferromagnetically. Frustration leads to non-trivial degeneracy of the ground state.

Spin frustration brings about interesting consequences for the resulting spin structures. As an example, let us consider three antiferromagnetically coupled spins located at each corner of a triangle. The stable spin configurations differ depending on the type of spin symmetry, or the number of spin components n. In the case of one-component Ising spins ($n = 1$), the ground state is not uniquely determined: the situation here is illustrated in figure 1. Frustration in the Ising case thus leads to non-trivial degeneracy of the ordered state.

By contrast, when the spin has a continuous symmetry as in the case of vector spins such as the two-component XY ($n = 2$) and the three-component Heisenberg ($n = 3$) spins, the ground-state spin configurations become *non-collinear* or *canted*, as illustrated in figure 2. Note that, in this case, frustration is partially released by mutual spin canting and there no longer remains a non-trivial degeneracy of the ground state up to global O(n) spin rotation and reflection. In this article, we shall concentrate on this latter type of frustrated magnet with non-collinear or canted ordered states.

1.2. Chirality

One interesting consequence of such canted spin structures is the appearance of a 'chiral' degree of freedom. Let us consider, for example, the case of XY spins shown in figure 2. If the exchange interactions are equal in magnitude on the three bonds, the ground-state spin configuration is the so-called '120° spin structure', in which three XY spins form 120° angles with the neighbouring spins. As shown in figure 2, the ground state of such triangular XY spins is twofold degenerate according to whether the resulting non-collinear spin structure is right- or left-handed (chiral degeneracy). A given chiral state cannot be transformed into the state with the opposite chirality via any global spin rotation in the XY-spin space, global spin *reflection* being required to achieve this. One may assign a *chirality* $+$ or $-$ to each

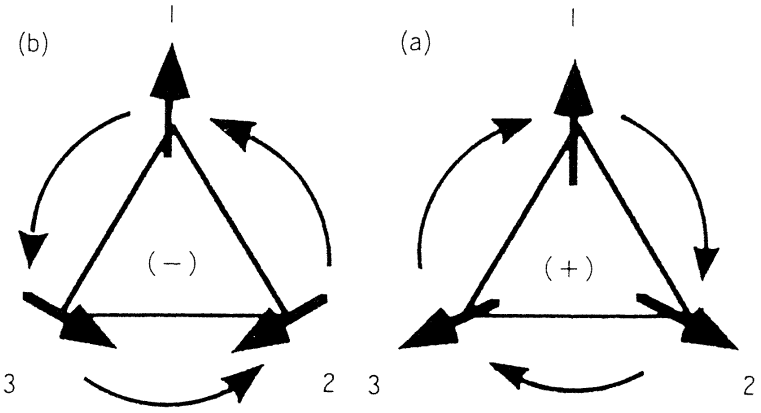

Figure 2. The ground-state spin configuration of three vector spins on a triangle coupled antiferromagnetically. Frustration leads to the non-collinear or canted ordered state. In the case of $n = 2$-component XY spins, the ground state is twofold degenerate according to whether the non-collinear spin structure is right- or left-handed, each of which is characterized by the opposite chirality as shown in (a) and (b).

of these two ground states. In other words, the ground-state manifold of the frustrated XY magnets possesses a hidden Ising-like discrete degeneracy, chiral degeneracy, in addition to a continuous degeneracy associated with the continuous XY-spin symmetry. The concept of chirality was introduced into magnetism first by Villain [1].

To characterize these two chiral states, it is convenient to introduce a scalar quantity, chirality, defined by [2]

$$\kappa_p = \frac{2}{3\sqrt{3}} \sum_{\langle ij \rangle}^{p} [\boldsymbol{S}_i \times \boldsymbol{S}_j]_z = \frac{2}{3\sqrt{3}} \sum_{\langle ij \rangle}^{p} (S_i^x S_j^y - S_i^y S_j^x) \tag{1.1}$$

where the summation runs over the three directed bonds surrounding a plaquette (triangle). One can easily confirm that κ_p gives ± 1 for the two spin configurations depicted in figure 2. Note that the chirality defined by (1.1) is a *pseudoscalar* in the sense that it is invariant under global spin rotation ($SO(2) = U(1)$) while it changes sign under global spin reflection (Z_2).

In the triangular spin structure formed by the $n = 3$-component Heisenberg spins, by contrast, there is no longer a discrete chiral degeneracy since the two spin configurations in

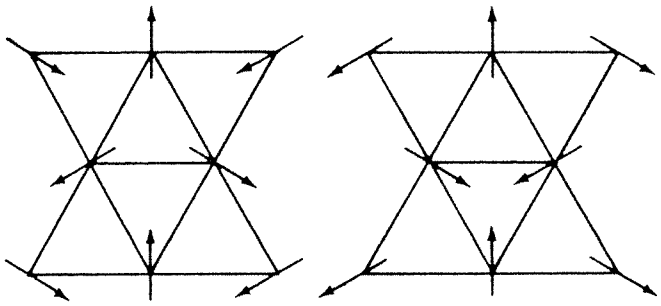

Figure 3. Chiral degeneracy in the ordered state of the XY antiferromagnet on the triangular lattice.

figure 2 can now be transformed into each other by continuous spin rotation via the third dimension of the Heisenberg spin. However, one can define a chirality *vector* as an axial vector defined by [3]

$$\boldsymbol{\kappa}_p = \frac{2}{3\sqrt{3}} \sum_{\langle ij \rangle}^{p} \boldsymbol{S}_i \times \boldsymbol{S}_j. \tag{1.2}$$

The situation described above is essentially the same also in the 2D triangular and 3D stacked-triangular antiferromagnets. In the ordered state, the sublattice-magnetization vector on each sublattice (the triangular layer consists of three interpenetrating triangular sublattices) cant with each other making an angle equal to 120°. In the case of XY spins, such triangular structure gives rise to chiral degeneracy as shown in figure 3.

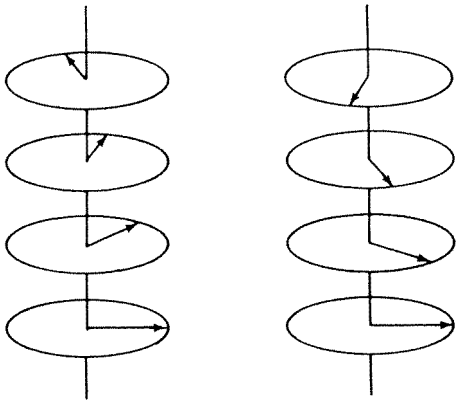

Figure 4. Chiral degeneracy in the ordered state of the XY helimagnet.

Similar chiral degeneracy is also realized in other types of canted magnet such as helimagnets (spiral magnets), in which right- and left-handed helices, as illustrated in figure 4, are energetically degenerate.

1.3. A short history of the research

Historically, studies on the critical properties of canted or non-collinear magnets were initiated more than 20 years ago for the rare-earth helimagnets Ho, Dy and Tb. In 1976, Bak and Mukamel analysed theoretically the critical properties of the paramagnetic–helimagnetic transition of the easy-plane-type (XY-like) helimagnets Ho, Dy and Tb [4]. Bak and Mukamel derived an effective Hamiltonian called the Landau–Ginzburg–Wilson (LGW) Hamiltonian appropriate for the XY ($n = 2$) helimagnet and performed a renormalization-group (RG) $\epsilon = 4 - d$ expansion analysis. They found a stable O(4)-like fixed point and claimed that Ho, Dy and Tb should exhibit a continuous transition characterized by the standard O(4)-like exponents $\alpha \simeq -0.17$, $\beta \simeq 0.39$, $\gamma \simeq 1.39$ and $\nu \simeq 0.70$. Note that the predicted singularity is weaker than that of the unfrustrated collinear XY magnet; that is, α is more negative while β, γ and ν are larger. Similar ϵ-expansion analysis with special attention paid to the effect of commensurability on the helical transition was also carried out by Garel and Pfeuty [5], who found, for the case of XY ($n = 2$) spins, the same O(4)-like fixed point as was obtained by Bak and Mukamel.

Meanwhile, experiments on the rare-earth helimagnets Ho, Dy and Tb gave somewhat inconclusive results. Some of these experiments, especially the neutron diffraction meas-

urements for Ho [6], supported the predicted O(4) behaviour, while some other experiments, such as the specific-heat measurements for Dy [7], Mössbauer measurements for Dy [8] and neutron diffraction measurements for Tb [9], yielded exponents significantly different from the O(4) values.

A few years later, Barak and Walker reanalysed the RG calculation by Bak and Mukamel, and found that the O(4)-like fixed point found by them was actually located in the region of the parameter space representing the *collinear* spin-density-wave (SDW) order, not the non-collinear helical order [10]. Since no stable fixed point was found in the appropriate region in the parameter space, Barak and Walker concluded that the paramagnetic–helimagnetic transition of Ho, Dy and Tb should be first order. Although most of the experimental work on Ho, Dy and Tb done so far has reported a continuous transition, a few authors suggested that the transition of Ho and Dy might actually be weakly first order [11, 12]. In fact, the experimental situation concerning the critical properties of these rare-earth helimagnets has remained confused for years now, in the sense that different authors reported significantly different exponent values, or even different orders of the transition, *for the same exponent of the same material*. For example, the reported values of the exponent β are scattered from 0.21 (Tb; x-ray) [13], 0.23 (Tb; neutron) [14], 0.25 (Tb; neutron) [9], 0.3 (Ho; neutron) [15], 0.335 (Dy; Mössbauer) [8], 0.37 (Ho; x-ray) [15], 0.38 (Dy; neutron) [16], 0.39 (Ho; neutron) [16, 18] to 0.39 (Dy; neutron) [17, 18].

In 1985–6, the first theoretical analysis of the critical properties of stacked-triangular antiferromagnets was made by the present author for the cases of *XY* and Heisenberg spins [19, 20]. By means of a symmetry analysis and Monte Carlo simulations, it was claimed that, due to its chiral degrees of freedom, the phase transition of these stacked-triangular antiferromagnets might be novel, possibly belonging to a new universality class, called the *chiral universality class*, different from the standard O(n) Wilson–Fisher universality class. The critical singularity observed in Monte Carlo simulations was stronger than that of the unfrustrated collinear *XY* and Heisenberg magnets, which is the opposite of Bak and Mukamel's O(4) prediction. Indeed, the exponent values determined by Monte Carlo simulations were $\alpha = 0.34 \pm 0.06$, $\beta = 0.253 \pm 0.01$, $\gamma = 1.13 \pm 0.05$ and $\nu = 0.54 \pm 0.02$ for the *XY* case, and $\alpha = 0.24 \pm 0.08$, $\beta = 0.30 \pm 0.02$, $\gamma = 1.17 \pm 0.07$ and $\nu = 0.59 \pm 0.02$ for the Heisenberg case [21]. It was predicted that such novel critical behaviour should be observed for the stacked-triangular *XY* antiferromagnet $CsMnBr_3$ ($n = 2$ chiral universality) [20, 22], and for the stacked-triangular Heisenberg antiferromagnets VCl_2 and VBr_2 ($n = 3$ chiral universality) [19, 22], while helimagnets such as Ho, Dy and Tb were also argued to exhibit the same novel $n = 2$ chiral critical behaviour asymptotically [20, 22]. RG analyses based on $\epsilon = 4 - d$ and $1/n$ expansions were also made by the author, and a new fixed point describing the non-collinear criticality was identified [23].

Stimulated by this theoretical prediction, several experiments were subsequently made on the critical properties of the stacked-triangular antiferromagnets $CsMnBr_3$, VCl_2 and VBr_2. The first experimental measurements of the critical properties of the stacked-triangular *XY* antiferromagnet $CsMnBr_3$ were performed by two groups, i.e., neutron scattering measurements by the McMaster group (Mason, Gaulin and Collins) [24] and those by the Japanese group (Ajiro, Kadowaki and co-workers) [25]. The results of these two independent measurements were consistent with each other and yielded exponent values close to the predicted values, giving some support to the chiral-universality scenario. Since then, further measurements have been performed on $CsMnBr_3$, including high-precision specific-heat measurements by the Santa Cruz group (Wang, Belanger and Gaulin) [26] and those by the Karlsruhe group (Deutschmann, Wosnitza, von Löhneysen and Kremer) [27]. For the stacked-triangular Heisenberg antiferromagnets VCl_2 and VBr_2, following the first

specific-heat measurements by Takeda and co-workers [28], both neutron scattering [29] and specific-heat [30] measurements were performed. Most of the exponents and specific-heat amplitude ratios obtained were in reasonable agreement with the predicted values.

By contrast, a more conservative view was proposed by Azaria, Delamotte and Jolicoeur a few years later [31, 32]. These authors studied a certain non-linear sigma model expected to describe the Heisenberg ($n = 3$) non-collinear or canted magnets based on the RG $\epsilon = d - 2$ expansion technique, and found a stable fixed point which was nothing but the standard O(4) Wilson–Fisher fixed point. These authors then suggested that the magnetic phase transition of non-collinear magnets, including both stacked-triangular antiferromagnets and helimagnets, might be of standard O(4) universality. The O(4) fixed point found there for the Heisenberg spins is different in nature from the O(4)-like fixed point found by Bak and Mukamel for the *XY* spins [4]: the former O(4) fixed point has no counterpart in the $\epsilon = 4 - d$ expansion. Azaria *et al* further speculated that the non-collinear transition could be either first order or mean-field tricritical depending on the microscopic properties of the system.

One useful method for directly testing those theoretical predictions is a Monte Carlo simulation on a simple spin model. Following the first Monte Carlo study on the *XY* and Heisenberg stacked-triangular antiferromagnets [19–21], extensive Monte Carlo simulations have been performed by several different groups, including the Saclay group (Bhattacharya, Billoire, Lacaze and Jolicoeur; Heisenberg) [33], the Cergy group (Loison, Boubcheur and Diep; *XY* [34] and Heisenberg [35]) and the Sherbrooke group (Mailhot, Plumer and Caillé; *XY* [36] and Heisenberg [37]). In the numerical sense, the results reported agreed with each other and with the earlier simulation of reference [21], except for a small difference remaining in some exponents of the *XY* system. More specifically, in the Heisenberg case, the results support the chiral-universality scenario in the sense that a continuous transition characterized by the novel exponents was observed in common. In particular, one may now rule out the possibility of the standard O(4) critical behaviour and of the mean-field tricritical behaviour predicted by Azaria *et al*. In the *XY* case, the results are again consistent with the chiral-universality scenario, but inconsistent with the O(4)-like behaviour predicted by Bak and Mukamel. Meanwhile, since the exponent values predicted for the $n = 2$ chiral universality are not very different from the mean-field tricritical values $\alpha = 0.5$, $\beta = 0.25$ and $\gamma = 1$, some authors interpreted their Monte Carlo results on the *XY* model as favouring mean-field tricritical behaviour rather than the chiral universality [36]. One should also bear in mind that the possibility of a weak first-order transition may not be completely ruled out by numerical simulations for finite lattices.

Important progress was also made in the study of the magnetic phase diagram and the multicritical behaviour of stacked-triangular antiferromagnets under external magnetic fields. In particular, a magnetic phase diagram with a novel multicritical point, different from those of the standard unfrustrated antiferromagnets, was observed by Johnson, Rayne and Friedberg for the weakly Ising-like stacked-triangular antiferromagnet $CsNiCl_3$ by means of susceptibility measurements [38]. For the stacked-triangular *XY* antiferromagnet $CsMnBr_3$, Gaulin, Mason, Collins and Larese revealed by means of neutron scattering measurements that the zero-field transition point corresponds to a tetracritical point in the magnetic field–temperature phase diagram [39]. These novel critical and multicritical properties of stacked-triangular antiferromagnets under external fields were theoretically investigated by Kawamura, Caillé and Plumer within a scaling theory based on the chiral-universality scenario, and several predictions were made [40]. To test these scaling prediction, further experiments were performed in turn, which revealed features of the non-collinear transitions under external fields.

1.4. Outline of the article

In the following sections, I wish to review in more detail these theoretical and experimental studies concerning the critical properties of non-collinear or canted magnets [41–44]. In section 2, I will introduce several typical magnetic materials exhibiting non-collinear spin order, and introduce simple spin models used in describing these non-collinear transitions. The LGW Hamiltonian appropriate for the non-collinear transitions is also introduced. In section 3, an intuitive symmetry argument is given on the basis of the notion of the order-parameter space. Symmetry properties of the LGW Hamiltonian are also examined. An analysis of topological defects in the non-collinearly ordered state is given, and the nature of topological phase transitions mediated by topological defects is briefly discussed. Section 4 is devoted to RG analyses of the non-collinear transitions, including $\epsilon = 4 - d$ expansion, $1/n$ expansion and $\epsilon = d - 2$ expansion. After the results of these RG calculations have been presented, several different theoretical proposals are explained and discussed. In section 5, the results of Monte Carlo simulations on the critical properties of *XY* and Heisenberg stacked-triangular antiferromagnets and of several related models are presented. In section 6, experimental results on the critical properties of both stacked-triangular antiferromagnets and helimagnets are reviewed. A possible experimental method for measuring the chirality is mentioned. The phase transition of stacked-triangular antiferromagnets under external magnetic fields is reviewed in section 7, with particular emphasis on the phase diagram and novel multicritical behaviour. Finally, in section 8, I summarize the present status of the study, and discuss future problems.

2. Materials and models

In this section, I introduce typical materials and model systems which have been used in the study of non-collinear phase transitions. These include both (a) stacked-triangular antiferromagnets and (b) helimagnets.

2.1. Stacked-triangular antiferromagnets

In stacked-triangular antiferromagnets, magnetic ions are located at each site of a three-dimensional stacked-triangular (simple hexagonal) lattice. Magnetic ions interact antiferromagnetically in the triangular layer, which causes geometry-induced frustration. The most extensively studied stacked-triangular antiferromagnets are ABX_3-type compounds, A standing for elements such as Cs and Rb, B standing for magnetic ions such as Mn, Cu, Ni and Co, and X standing for halogens such as Cl, Br and I [42, 44]. While these materials are magnetically quasi-one-dimensional ones, it has been established that most of them exhibit a magnetic transition to a three-dimensionally ordered state at low temperatures with sharp magnetic Bragg peaks. There are a rich variety of materials for the various combinations of the constituent ions, A, B and X [44].

Crucial to the nature of the phase transition is the type of the magnetic anisotropy. Some of these compounds are Ising-like with easy-axis-type (or axial) anisotropy, some are *XY*-like with easy-plane-type (or planar) anisotropy and others are Heisenberg-like with negligibly small anisotropy. In zero field, the non-collinear criticality is realized in the *XY* and Heisenberg systems, which include $CsMnBr_3$, $CsVBr_3$ (*XY*), $CsVCl_3$ and $RbNiCl_3$ (nearly Heisenberg). By contrast, the Ising-like axial magnets, including $CsNiCl_3$, $CsNiBr_3$ and $CsMnI_3$, often exhibit two successive phase transitions in zero field with a collinearly ordered intermediate phase. If an external field of appropriate intensity is applied along an

easy axis, however, a direct transition from the paramagnetic state to the non-collinearly ordered state becomes possible. Such a transition in an external field is characterized by non-trivial chirality, and will also be discussed later in section 6 and section 7.

Quasi-two-dimensional realizations of stacked-triangular antiferromagnets may include the vanadium compounds VX_2 with X = Cl and Br. VX_2 is a nearly isotropic (Heisenberg-like) magnet with weak Ising-like anisotropy. While VX_2 exhibits two successive transitions at two distinct but mutually close temperatures due to the weak easy-axis-type anisotropy ($T_{N1} \simeq 35.88$ K and $T_{N2} \simeq 35.80$ K in the case of VCl_2 [29]), it is expected to behave as an isotropic Heisenberg system except close to T_{N1} or T_{N2}.

Since our interest is in non-collinear criticality, we will mainly be concerned in this article with vector-spin systems, including both $n = 2$-component XY and $n = 3$-component Heisenberg spin models. A simple vector-spin Hamiltonian often used in modelling such stacked-triangular antiferromagnets may be given by

$$\mathcal{H} = -J \sum_{\langle ij \rangle} \boldsymbol{S}_i \cdot \boldsymbol{S}_j - J' \sum_{\langle\langle ij \rangle\rangle} \boldsymbol{S}_i \cdot \boldsymbol{S}_j \tag{2.1}$$

where $\boldsymbol{S}_i = (S_i^{(1)}, S_i^{(2)}, \ldots, S_i^{(n)})$ is an n-component unit vector with $|\boldsymbol{S}_i| = 1$ located at the ith site of a stacked-triangular lattice, while $J < 0$ and J' represent the intraplane and interplane nearest-neighbour couplings. The first sum is taken over all nearest-neighbour pairs in the triangular layer, while the second sum is taken over all nearest-neighbour pairs along the chain direction orthogonal to the triangular layer.

2.2. Helimagnets

The second class of non-collinear magnets is the helimagnets or spiral magnets. Examples include β-MnO_2 and the rare-earth metals Ho, Dy and Tb. The rare-earth helimagnets Ho, Dy and Tb crystallize into the hexagonal-close-packed (hcp) structure, and form magnetic spirals along the c-axis below T_N with the moments lying in the basal plane. The interaction between the magnetic moments is the long-range Ruderman–Kittel–Kasuya–Yoshida (RKKY) interaction which falls off as $1/r^3$ and oscillates in sign with distance r. The oscillating nature of the RKKY interaction leads to frustration between the near-neighbour and further-neighbour interactions which stabilizes the non-collinear helical spin structure.

A simple model Hamiltonian which gives rise to a spiral structure is the axial-next-nearest-neighbour XY or Heisenberg model on a simple cubic lattice, with the ferromagnetic (or antiferromagnetic) nearest-neighbour interaction in all directions and the antiferromagnetic next-nearest-neighbour interaction along one particular direction, say the x-direction. The Hamiltonian may be written as

$$\mathcal{H} = -J_1 \sum_{\langle ij \rangle} \boldsymbol{S}_i \cdot \boldsymbol{S}_j - J_2 \sum_{\langle\langle ij \rangle\rangle} \boldsymbol{S}_i \cdot \boldsymbol{S}_j \tag{2.2}$$

where the first sum is taken over all nearest-neighbour pairs on the lattice while the second sum is taken over next-nearest-neighbour pairs along the x-direction. The competition between the nearest-neighbour interaction J_1 and the antiferromagnetic axial next-nearest-neighbour interactions $J_2 < 0$ gives rise to a magnetic spiral along the x-direction when the value of $|J_2/J_1|$ exceeds a certain critical value.

One difference between such spiral structure and the non-collinear structure in the stacked-triangular antiferromagnet is that the pitch of the helix is generally incommensurate with the underlying lattice, in contrast to the 120° spin structure which is always commensurate with the underlying lattice. (In fact, one can generate the incommensurate

spin structure even in stacked-triangular antiferromagnets, e.g., by breaking the equivalence of the intraplane couplings [45, 46]. This case might have some relevance to the incommensurate spin order in $RbMnBr_3$ as will be discussed in section 6.)

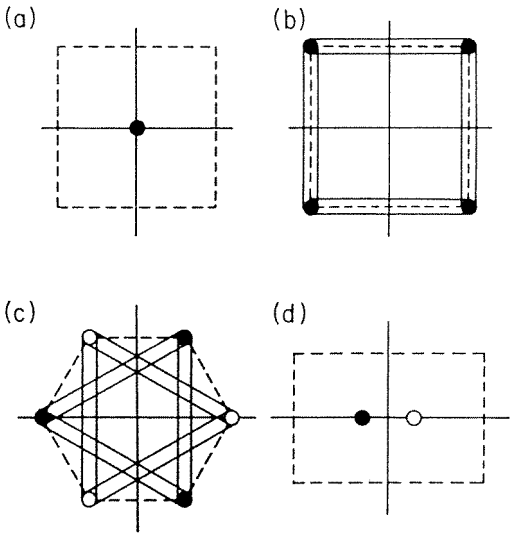

Figure 5. Representations of 'instability points', solid and open circles, in wavevector space for (a) ferromagnets, (b) antiferromagnets on bipartite lattices, (c) stacked-triangular antiferromagnets and (d) helimagnets. The dashed lines outline the first Brillouin zone. Double lines represent the reciprocal-lattice vectors $\boldsymbol{K}$: as usual, points connected by a vector $\boldsymbol{K}$ should be fully identified.

2.3. The Landau–Ginzburg–Wilson (LGW) Hamiltonian

The spin Hamiltonians (2.1) and (2.2) have been written in terms of spin variables of fixed length, $|\boldsymbol{S}_i| = 1$. In some of the RG analyses such as $\epsilon = 4 - d$ or $1/n$ expansions, an alternative form of Hamiltonian written in terms of spin variables of unconstrained length is often used. It is given in the form of an expansion in order-parameter fields (critical modes), and is called the Landau–Ginzburg–Wilson (LGW) Hamiltonian. In the case of standard ferromagnets or unfrustrated collinear antiferromagnets, an appropriate LGW Hamiltonian is the so-called ϕ^4-model whose Hamiltonian density is given by

$$\mathcal{H}_{\mathrm{LGW}} = \frac{1}{2}[(\nabla\boldsymbol{\phi})^2 + r\boldsymbol{\phi}^2 + u\boldsymbol{\phi}^4] \tag{2.3}$$

where the n-component vector field $\boldsymbol{\phi} = (\phi_1, \phi_2, \ldots, \phi_n)$ represents a near-critical mode around an instability point. In unfrustrated ferromagnets or antiferromagnets, the instability occurs only at one point in the wavevector space, as shown in figures 5(a) and 5(b). Therefore, a single n-vector field $\boldsymbol{\phi}$ is sufficient for describing the phase transition.

By contrast, in the case of non-collinear or canted magnets such as stacked-triangular antiferromagnets or helimagnets, the instability occurs simultaneously at two distinct points in the wavevector space. Therefore, two equivalent but distinct n-component vector fields are needed to describe the associated phase transition. The situation is illustrated in figures 5(c) and 5(d) for the cases of stacked-triangular antiferromagnets and helimagnets, respectively. These two instability modes may be taken as the Fourier modes at $\pm\boldsymbol{Q}$,

where $\boldsymbol{Q} = (4\pi/3, 0, 0, \ldots, 0)$ for the case of stacked-triangular antiferromagnets and $\boldsymbol{Q} = (2\pi/\lambda, 0, 0, \ldots, 0)$ for the case of helimagnets, λ being the pitch of the helix. It is convenient for later use to extend the model to general d spatial dimensions. In the case of stacked-triangular antiferromagnets, the lattice is then regarded as two-dimensional triangular layers stacked in hypercubic fashion along the remaining $d-2$ directions, while in the case of helimagnets, the competing second-neighbour interaction is assumed to work only along the first direction in d dimensions, along which the helix is formed.

One can derive the soft-spin LGW Hamiltonian starting from the microscopic hard-spin Hamiltonian (2.1) or (2.2) by a series of transformations [23]. By softening the fixed-length spin condition, Fourier transforming and retaining only near-critical models, one obtains

$$\mathcal{H}_{\mathrm{LGW}} = \frac{1}{2}[(\nabla \boldsymbol{a})^2 + (\nabla \boldsymbol{b})^2 + r(\boldsymbol{a}^2 + \boldsymbol{b}^2) + u(\boldsymbol{a}^2 + \boldsymbol{b}^2)^2 + v\{(\boldsymbol{a}\cdot\boldsymbol{b})^2 - \boldsymbol{a}^2\boldsymbol{b}^2\}] \tag{2.4}$$

where $\boldsymbol{a}$ and $\boldsymbol{b}$ are n-component vector fields representing the cosine and sine components associated with the non-collinear spin structure at wavevectors $\pm\boldsymbol{Q}$ via

$$\boldsymbol{S}(\boldsymbol{r}) = \boldsymbol{a}(\boldsymbol{r})\cos(\boldsymbol{Q}\cdot\boldsymbol{r}) + \boldsymbol{b}(\boldsymbol{r})\sin(\boldsymbol{Q}\cdot\boldsymbol{r}). \tag{2.5}$$

In order for the spin structure (2.5) to really represent the non-collinear order, the $\boldsymbol{a}$- and $\boldsymbol{b}$-fields must be orthogonal to each other. This requires that the quartic coupling v in the LGW Hamiltonian (2.4) should be positive. If v is negative, on the other hand, the spin structure given by (2.5) represents the collinearly ordered SDW state (or the sinusoidal state). The LGW Hamiltonian (2.4) forms a basis of the following RG analysis based on $\epsilon = 4-d$ and $1/n$ expansions.

In the particular case of XY ($n = 2$) spins, one can transform equation (2.4) into a different form [23]:

$$\mathcal{H}_{\mathrm{LGW}} = \frac{1}{2}\Bigg[(\nabla \boldsymbol{A})^2 + (\nabla \boldsymbol{B})^2 + r(\boldsymbol{A}^2 + \boldsymbol{B}^2) + \left(u - \frac{1}{4}v\right)(\boldsymbol{A}^4 + \boldsymbol{B}^4) + 2\left(u + \frac{1}{4}v\right)\boldsymbol{A}^2\boldsymbol{B}^2\Bigg] \tag{2.6}$$

where $\boldsymbol{A}$ and $\boldsymbol{B}$ are two-component fields defined by

$$\begin{aligned} A_x &= (a_x + b_y)/\sqrt{2} \qquad & B_x &= (a_y + b_x)/\sqrt{2} \\ A_y &= (a_y - b_x)/\sqrt{2} \qquad & B_y &= (-a_x + b_y)/\sqrt{2}. \end{aligned} \tag{2.7}$$

The RG analysis of reference [4] was performed on the basis of the form (2.6), rather than (2.4). From (2.6), it is easy to see that, in the case of $n = 2$, the model reduces to two decoupled XY models on the special manifold $v = -4u$. Note that this manifold lies in the sinusoidal region, $v < 0$.

Essentially the same LGW Hamiltonian has also been used in other problems such as that of the phase transition of the dipole-locked A phase of helium three [47, 48], the superconducting phase transition of the heavy-fermion superconductor UPt_3 [49] and the quantum phase transition of a certain Josephson junction array in a magnetic field [50].

3. Symmetry

3.1. Symmetry of the ordered state

Because of its non-trivial chiral degrees of freedom, the ordered state of frustrated non-collinear magnets has a symmetry that differs from that of unfrustrated collinear magnets.

Let us consider, for example, the case of the $n = 3$-component Heisenberg spins. In the unfrustrated collinear case, spins align parallel or antiparallel with each other forming the collinear ground state. One can see that such a ground state is invariant under global spin rotation around the magnetization (or the sublattice-magnetization) axis. In the frustrated non-collinear case, by contrast, the 120° spin structure does not have such an invariance. Therefore, symmetries of the ordered states are clearly different in the collinear and the non-collinear cases. Obviously, the conventional index n, the number of the spin components, is inadequate for distinguishing between such differences in the symmetry of the ordered states.

In order to characterize the relevant symmetry, it is convenient to introduce the notion of order-parameter space, which is a topological space isomorphic to the set of ordered states [51]. In the collinear case, the order-parameter space V may be represented by a single arrow in the three-dimensional spin space and is isomorphic to the two-dimensional sphere S_2 (the surface of a ball in Euclidean three-space). In the non-collinear case, the order-parameter space cannot be represented by a single arrow. Instead, additional structure caused by non-collinear alignment of spins leads to an order-parameter space isomorphic to the three-dimensional rotation group SO(3), or equivalently, to the projective space P_3 [3]. In the collinear case, rotation invariance around the magnetization axis reduces the order-parameter space to $V = SO(3)/SO(2) = S_2$.

In the case of the $n = 2$-component XY spins, the order-parameter space of unfrustrated collinear systems is $V = S_1 = SO(2)$, while that of frustrated non-collinear systems is $V = Z_2 \times S_1 = Z_2 \times SO(2) = O(2)$ where Z_2 pertains to the aforementioned twofold chiral degeneracy while $S_1 = SO(2)$ pertains the rotation symmetry of the original XY spins.

Order-parameter space may also be defined as a topological space obtained by dividing the whole symmetry group of the Hamiltonian, which we assume to be $O(n)$, by the subgroup which keeps the ordered state (the symmetry-broken state) unchanged [51]. With the use of this definition, one can easily generalize the argument to the general $n \geqslant 2$-component vector spins. In the unfrustrated collinear case, the invariant subgroup turns out to be $O(n-1)$, consisting of the rotation around the magnetization axis. This leads to the associated order-parameter space isomorphic to the $(n-1)$-dimensional hypersphere, $V = O(n)/O(n-1) = SO(n)/SO(n-1) = S_{n-1}$. In the particular cases of $n = 2$ or 3, this simply reproduces the results mentioned above.

In the frustrated non-collinear case, if one notes that the 120° spin structure spans the two-dimensional subspace in n-dimensional spin space, one may see that the invariant subgroup is $O(n-2)$ rather than $O(n-1)$. Thus, the order-parameter space for the $n \geqslant 2$-component non-collinear systems is isomorphic to the Stiefel manifold, $V = O(n)/O(n-2)$ [41]. In the $n = 2$ case, it reduces to $V = O(2)$ since $O(0) = 1$, whereas in the $n = 3$ case, it reduces to $V = SO(3)$ since $O(1) = Z_2$.

Thus, the difference in the symmetry of the ordered states can be described in topological terms as the difference in the associated order-parameter spaces. Since the symmetry of the ordered state is a crucial ingredient of the corresponding disordering phase transition, this observation strongly suggests that the frustrated non-collinear magnets might exhibit a novel phase transition, possibly belonging to a new universality class [19, 20]. Of course, another possibility might be that these non-collinear magnets exhibit a first-order transition. One cannot even rule out the possibility that the symmetry is dynamically restored at the transition, and that the non-collinear transition is in the conventional Wilson–Fisher universality class. In order to determine which of the above possibilities is actually the case, more detailed analysis is needed. Still, the fact that one obtains for frustrated non-

collinear magnets an order-parameter space different from that for the unfrustrated collinear magnets gives a hint that something new may happen in the non-collinear transitions.

3.2. The symmetry of the LGW Hamiltonian

Next, let us examine the symmetry properties of the LGW Hamiltonian of non-collinear magnets with n-component spins, equation (2.4). The LGW Hamiltonian is invariant under the following two symmetry transformations: (i) O(n) spin rotation, $\boldsymbol{a}' = R\boldsymbol{a}$, $\boldsymbol{b}' = R\boldsymbol{b}$ with $R \in \mathrm{O}(n)$, as well as (ii) O(2) phase rotation, $\boldsymbol{a}' = (\cos\theta)\boldsymbol{a} - (\sin\theta)\boldsymbol{b}$, $\boldsymbol{b}' = \pm((\sin\theta)\boldsymbol{a} + (\cos\theta)\boldsymbol{b})$ [23]. The latter invariance arises from the arbitrariness in choosing the phase and the handedness of the two basis vectors.

Conversely, the symmetry requirements (i) and (ii) fully determine the form of the Hamiltonian up to quartic order in the fields $\boldsymbol{a}$ and $\boldsymbol{b}$ as given in (2.4). One may easily see that this O(n) $\times$ O(2) symmetry of the LGW Hamiltonian just corresponds to the aforementioned order-parameter space $V = \mathrm{O}(n)/\mathrm{O}(n-2)$.

In the case of $n = 2$, and in this case only, the LGW Hamiltonian (2.4) has a discrete symmetry, independent of the above O(n) $\times$ O(2) symmetry. This corresponds to a permutation of the field variables, namely (iii) ($a_x' = a_x, a_y' = b_x, b_x' = a_y, b_y' = b_y$) or ($a_x' = b_y, a_y' = a_y, b_x' = b_x, b_y' = a_x$).

3.3. Classification of topological defects

One property which can be determined solely from the topological considerations is the classification of topological defects in the ordered state. Although we do not give the details of the method (for these, see reference [51]), the point is that one can obtain all possible topological defects together with their 'topological quantum number' from the knowledge of its order-parameter space V by examining its rth homotopy group, $\Pi_r(V)$.

Table 1. Order-parameter spaces and the associated homotopy groups for various continuous spin systems in two dimensions.

	V	$\Pi_0(V)$	$\Pi_1(V)$	$\Pi_2(V)$
Defect	—	Line	Point	Instanton
Collinear *XY*	$\mathrm{S}_1 = \mathrm{SO}(2)$	0	Z	0
Collinear Heisenberg	S_2	0	0	Z
Non-collinear *XY*	$\mathrm{Z}_2 \times \mathrm{S}_1 = \mathrm{O}(2)$	Z_2	Z	0
Non-collinear Heisenberg	SO(3)	0	Z_2	0

Topological defects play an essential role in the phase transition of two-dimensional systems. Many two-dimensional phase transitions, such as the Kosterlitz–Thouless transition, are known to be 'defect mediated' [52]. The classification of topological defects in the collinear and non-collinear $d = 2$-dimensional magnets is given in table 1 for the cases of *XY* ($n = 2$) and Heisenberg ($n = 3$) spins [3].

The non-collinear 2D *XY* systems, such as the triangular-lattice *XY* antiferromagnets and the Josephson-junction arrays in a magnetic field, possess the standard Kosterlitz–Thouless-type vortex characterized by the integral topological quantum number Z as well as the chiral domain wall characterized by the two-valued topological quantum number Z_2. The vortex (point defect) is related to the continuous *XY* degrees of freedom via the relation $\Pi_1(\mathrm{S}_1) = \mathrm{Z}$, while the domain wall (line defect) is related to the discrete chiral

degrees of freedom via the relation $\Pi_0(Z_2) = Z_2$. Since earlier MC work on the triangular *XY* antiferromagnet by Miyashita and Shiba [2] and by Lee *et al* [53], and that on the Josephson-junction array by Teitel and Jayaprakash [54], many numerical studies have been made with special attention paid to how these two degrees of freedom order. While the existence of a phase transition with a sharp specific-heat anomaly driven by the appearance of the chiral long-range order has been established, the question of whether the spin and the chirality order at the same temperature, or at two close but distinct temperatures, still remains somewhat controversial [55, 56].

As was first observed by Kawamura and Miyashita [3], non-collinear Heisenberg magnets, such as the triangular Heisenberg antiferromagnet, possess a peculiar vortex characterized by its quantum number Z_2 (the Z_2 vortex), different in nature from the standard Z vortex of the *XY* magnets. Although it is generally believed that the two-dimensional Heisenberg model does not exhibit any phase transition at finite temperature [57], the possible existence of a novel topological phase transition mediated by these Z_2 vortices in the two-dimensional triangular Heisenberg antiferromagnet was suggested by Kawamura and Miyashita [3]. The predicted low-temperature phase is an exotic spin-liquid phase where the two-point spin correlation decays exponentially and the spin-correlation length remains finite. A quantity called the vorticity modulus, characterizing such exotic vortex order not accompanying the conventional spin order, was proposed and calculated [58, 59].

In three spatial dimensions, our main concern here, point defects in two dimensions appear as line defects. Hence, non-collinear *XY* magnets in $d = 3$ dimensions possess Z-vortex lines in addition to the Z_2 chiral domain walls, while the non-collinear Heisenberg magnets possess Z_2-vortex lines. Although it is possible and enlightening to envisage the nature of the three-dimensional transitions also as defect mediated [60], we follow more standard theoretical approaches in this article in which these topological defects do not show up in an explicit way.

4. Theoretical analysis of the critical properties—renormalization-group analysis

In this section, I will review the theoretical analysis of the critical properties of non-collinear transitions on the basis of several renormalization-group (RG) methods in some detail, including $\epsilon = 4 - d$ expansion, $1/n$ expansion and $\epsilon = d - 2$ expansion.

4.1. Mean-field approximation

Standard RG calculations such as $\epsilon = 4 - d$ and $1/n$ expansions are generally performed on the basis of the soft-spin LGW Hamiltonian. Before entering into the RG analysis, it may be instructive here to summarize the results of the standard mean-field approximation applied to the LGW Hamiltonian, equation (2.4) [23].

When the quartic coupling constant v is positive and satisfies the inequality $v < 4u$, a continuous transition takes place at $r = 0$ between the paramagnetic and the non-collinear states, characterized by

$$|\boldsymbol{a}|^2 = |\boldsymbol{b}|^2 = -r/(4u - v) \qquad \boldsymbol{a} \perp \boldsymbol{b} \qquad (0 < v < 4u). \tag{4.1a}$$

When v is negative, by contrast, there is a continuous transition at $r = 0$ between the paramagnetic and the collinearly ordered sinusoidal states characterized by

$$|\boldsymbol{a}|^2 + |\boldsymbol{b}|^2 = -r/2u \qquad \boldsymbol{a} \parallel \boldsymbol{b} \qquad (v < 0). \tag{4.1b}$$

Note that, in the sinusoidal case, the relative magnitude of $\boldsymbol{a}$ and $\boldsymbol{b}$ is not determined: this corresponds physically to the sliding degree of freedom of the spin-density wave.

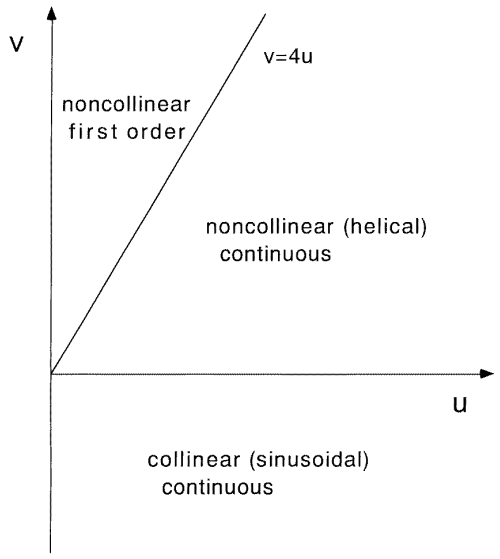

Figure 6. The mean-field phase diagram in the (u, v) plane of the LGW Hamiltonian (2.4), where u and v are two quartic coupling constants. On the line $v = 4u$, the transition to the non-collinear state is mean-field tricritical.

Stability of the free energy requires the conditions

$$u > 0 \qquad v < 4u. \tag{4.2}$$

When $u < 0$ or $v > 4u$, a higher-order (sixth-order) term is necessary to stabilize the free energy, and the transition in such a case generally becomes *first order*. The mean-field phase diagram in the u–v plane is summarized in figure 6. Continuous transitions are characterized by the standard mean-field exponents, $\alpha = 0$, $\beta = 1/2$ and $\gamma = 1$ etc, while the mean-field tricritical exponents $\alpha = 1/2$, $\beta = 1/4$ and $\gamma = 1$ etc are realized along the stability boundary $v = 4u$. Of course, fluctuations generally change these conclusions, as we shall see below.

4.2. $\epsilon = 4 - d$ expansion

In this subsection, I will review the results of the RG $\epsilon = 4 - d$ expansion for the non-collinear transition. Earlier attempts were made for XY ($n = 2$) helimagnets to $O(\epsilon^2)$ by Bak and Mukamel [4], and later by Barak and Walker [10], with special attention paid to the paramagnetic–helimagnetic transition of the rare-earth metals Ho, Dy Tb. Similar $O(\epsilon^2)$ analysis for general n-component helimagnets was carried out by Garel and Pfeuty with special attention paid to the possible effect of commensurability on the helical transition [5], and by Jones, Love and Moore [47] and by Bailin, Love and Moore [48] in the context of the superfluidity transition of helium three. A fuller analysis in the light of a possible new universality class was made by the present author [23]. More recently, a higher-order calculation to $O(\epsilon^3)$ was carried out by Antonenko, Sokolov and Varnashev [61]. Since the results obtained were sometimes interpreted in different ways by these authors, I will postpone the discussion of their physical implications to later subsections and will first present the results based on references [23] and [61].

4.2.1. The RG flow diagram, fixed points and critical exponents. Let us consider the LGW Hamiltonian for general n-component non-collinear magnets, equation (2.4). Its upper critical dimension is $d_> = 4$ and a standard RG $\epsilon = 4 - d$ expansion can be performed. Near four dimensions, there are up to *four* fixed points depending on the value of n. Two exist for all n: one is the trivial Gaussian field point located at the origin ($u^* = v^* = 0$), which is always unstable against both u- and v-perturbations; the other corresponds to the conventional isotropic O($2n$) Heisenberg fixed point at ($u^* > 0, v^* = 0$), which is stable for sufficiently small n. To describe the remaining fixed points, we consider four distinct regimes for relating n and d.

(I) $n > n_{\rm I}(d) = 12 + 4\sqrt{6} - [(36 + 14\sqrt{6})/3]\epsilon + [\frac{137}{150} + \frac{91}{300}\sqrt{6} + (\frac{13}{5} + \frac{47}{60}\sqrt{6})\zeta(3)]\epsilon^2 + \mathrm{O}(\epsilon^3) \simeq 21.8 - 23.4\epsilon + 7.1\epsilon^2 + \mathrm{O}(\epsilon^3)$.

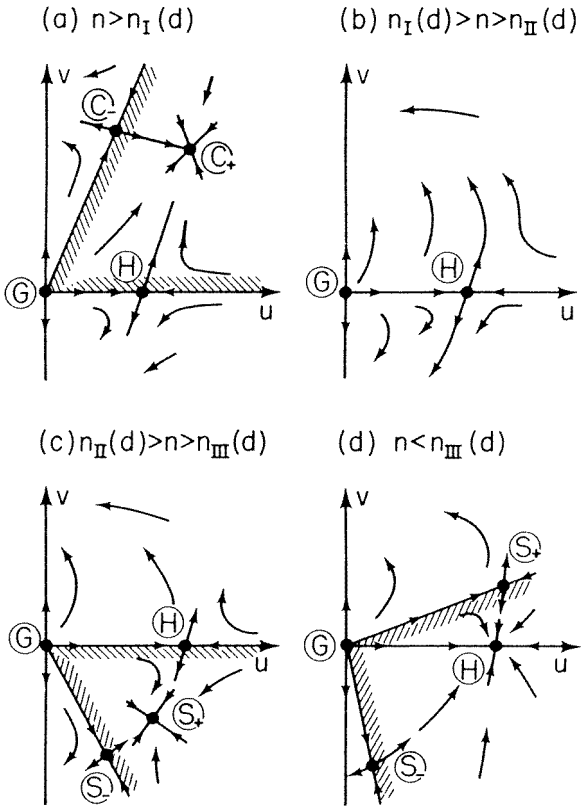

Figure 7. Renormalization-group flows in the (u, v) plane obtained from the $\epsilon = 4-d$ expansion for the LGW Hamiltonian (2.4). Parts (a)–(d) correspond to the regimes I–IV specified in the text. The hatched regions represent basins of attraction of the stable fixed point. In (a), the line connecting the Gaussian fixed point G and the unstable antichiral fixed point C_- is the tricritical line corresponding to the separatrix between the two regions in the parameter space, one associated with a continuous transition (the hatched region) and the other with a first-order transition.

When n is sufficiently large to meet this condition, two new fixed points appear in the non-collinear region $v > 0$. They may be termed *chiral*, C_+, and *antichiral*, C_-, the former being stable in accord with the RG flow sketched in figure 7(a). When n approaches $n_{\rm I}(d)$,

the chiral and antichiral fixed points coalesce at a point in the upper (u, v) half-plane and become complex valued for $n < n_{\rm I}(d)$. In the sinusoidal region, $v < 0$, no stable fixed points are found.

(II) $n_{\rm I}(d) > n > n_{\rm II}(d) = 12 - 4\sqrt{6} - [(36 - 14\sqrt{6})/3]\epsilon + [\frac{137}{150} - \frac{91}{300}\sqrt{6} + (\frac{13}{5} - \frac{47}{60}\sqrt{6})\zeta(3)]\epsilon^2 + {\rm O}(\epsilon^3) \simeq 2.20 - 0.57\epsilon + 0.99\epsilon^2 + {\rm O}(\epsilon^3)$.

The RG flows are now as depicted in figure 7(b). Only the Gaussian and Heisenberg fixed points are present and both are unstable. Consequently, the transition to both non-collinear and sinusoidal phases is expected to be first order.

(III) $n_{\rm II}(d) > n > n_{\rm III}(d) = 2 - \epsilon + \frac{5}{24}(6\zeta(3) - 1)\epsilon^2 + {\rm O}(\epsilon^3) \simeq 2 - \epsilon + 1.3\epsilon^2 + {\rm O}(\epsilon^3)$.

In this regime, a new pair of fixed points appear in the sinusoidal region, $v < 0$, which may be termed *sinusoidal*, S_+, and *antisinusoidal*, S_-. The corresponding flows resemble those sketched in figure 7(c). The fixed point S_+ is the fixed point identified by Bak and Mukamel [4], and by Garel and Pfeuty [5], as a physical fixed point governing the *XY* ($n = 2$) helimagnets for $d = 3$. In the case of $n = 2$, S_+ coincides to ${\rm O}(\epsilon)$ with the O(4) fixed point, H, on the $v = 0$ axis, while it moves to the lower half-plane at higher order in ϵ. Thus, S_+ is the O(4)-like fixed point to ${\rm O}(\epsilon^2)$ in the sense that all exponents agree with the isotropic O(4) exponents, but it is not exactly an O(4) fixed point as can be confirmed by higher-order calculation [62]. In any case, this Bak and Mukamel fixed point is located in the sinusoidal region $v < 0$, and cannot be invoked to describe the non-collinear phase transitions [10]. As $n \to n_{\rm III}(d)$, the sinusoidal fixed point S_+ approaches the $v = 0$ axis and, at $n = n_{\rm III}(d)$, it meets the Heisenberg fixed point H and exchanges stability with it. In the non-collinear region $v > 0$, no stable fixed point exists.

(IV) $n > n_{\rm III}(d)$.

As illustrated in figure 7(d), the unstable fixed point S_+ now lies above the $v = 0$ axis. The Heisenberg fixed point H is stable and governs the critical behaviour of regions of both non-collinear and sinusoidal ordered behaviour.

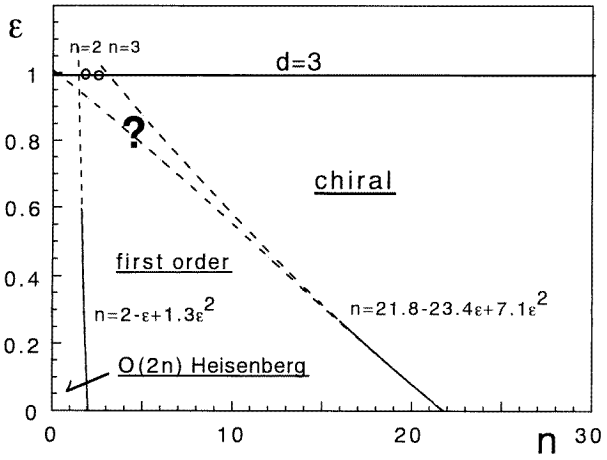

Figure 8. Stability regions in the (n, d) plane, with $\epsilon = 4 - d$, of fixed points accessible in the non-collinear region $v > 0$.

In view of the above four cases, one can see that, in the non-collinear region $v > 0$, the stable fixed point describing the non-collinear transition is either the chiral fixed point C_+,

which is stable for sufficiently large n:

$$n > n_1(d) = 21.8 - 23.4\epsilon + 7.1\epsilon^2 + \mathrm{O}(\epsilon^3) \tag{4.3}$$

or the O($2n$) Heisenberg fixed point H, stable for sufficiently small $n < n_{\mathrm{III}}(d)$. At these stable fixed points, critical exponents can be calculated in the standard manner. The exponents at the standard Heisenberg fixed point are well known, while the ones at the chiral fixed point are new. To the lowest order, the exponents γ and ν at the chiral fixed point were calculated as [23]

$$\gamma \approx 2\nu = 1 + \frac{n(n^2+n+48)+(n+4)(n-3)\sqrt{n^2-24n+48}}{4(n^3+4n^2-24n+144)}\epsilon + \mathrm{O}(\epsilon^2). \tag{4.4}$$

These γ and ν are numerically smaller than the corresponding O(n) Heisenberg values. The critical-point decay exponent to O(ϵ^2) was calculated as [23]

$$\eta = \frac{n(n^2+n+48)+(n+4)(n-3)\sqrt{n^2-24n+48}}{4(n^3+4n^2-24n+144)}\epsilon^2 + \mathrm{O}(\epsilon^3). \tag{4.5}$$

For the non-collinear region $v > 0$, the facts concerning the stable fixed points are summarized in figure 8.

The crucial question is that of what happens at the physically significant points, i.e. where $\epsilon = 1$ ($d = 3$) with $n = 2$ and 3. Unfortunately, these are rather far from the $\epsilon \to 0$ limit and, thus, it is very difficult to obtain a truly definitive answer from the ϵ-expansion with only a few terms. In fact, different authors gave different conjectures. The existence of the chiral fixed point C_+ was first noticed for large enough n ($n > 21.8$) by Moore and co-workers in references [46] and [47] in the context of helium three, while these authors claimed that the transition in the physical case ($n = 3$, $d = 3$) was first order since $n = 3$ was significantly smaller than 21.8. A detailed study of the chiral fixed point, including the ϵ-expansion expression for the stability boundary $n_1(d)$, was first carried out in reference [23], where it was argued in view of the Monte Carlo results that the chiral fixed point might remain stable down to $n = 2$ or 3 for $d = 3$. In contrast, Antonenko, Sokolov and Varnashev claimed on the basis of their O(ϵ^2) expression of $n_1(d)$ and its Borel–Padé resummation that the transition for $d = 3$ was first order for both $n = 2$ and $n = 3$ [61].

Instead of the $\epsilon = 4 - d$ expansion where the dimension d is expanded in powers of ϵ, one can perform the RG loop expansion directly at $d = 3$. This was also done by Antonenko and Sokolov to three-loop order, yielding results similar to those of the ϵ-expansion calculation to the same order [63].

Note also that, if one makes the standard ϵ-expansion fixing n at $n = 2$ or 3 (or any value smaller than 21.8), the chiral fixed point can never be seen [4]. This is simply because the ϵ-expansion method can detect only the type of fixed point which exists, stable or unstable, in the $\epsilon \to 0$ limit.

In the special case of XY ($n = 2$) sinusoidal ordering $v < 0$, one can give a non-perturbative argument to identify the stable fixed point for $d = 3$, making use of the fact that the system reduces to the decoupled XY models on the line $v = -4u$. In the XY case, the fixed point S_- is located on this $v = -4u$ line and becomes the standard XY fixed point (the O(2) Wilson–Fisher fixed point). One can then show, on the basis of a non-perturbative argument, that this XY fixed point is stable for $d = 3$ [64]. This is in contrast to the behaviour obtained from the low-order ϵ-expansion as sketched in figure 7(c), where the fixed point S_- is unstable [61, 62, 65]. Unfortunately, this discrepancy between the low-order ϵ-expansion result and the non-perturbative result cannot be remedied even

if one goes to higher order, say to $O(\epsilon^3)$, and carries out a resummation procedure [62]. This observation gives us a warning that one should not place too much trust in the result from the $\epsilon = 4 - d$ expansion in some subtle cases, even when a relatively higher-order calculation, say to $O(\epsilon^3)$, was performed together with the resummation technique.

4.2.2. Chirality and other composite operators. In this subsection, we show how the chirality, defined in section 1.2 as a quantity characterizing the non-collinear spin structure, manifests itself in the RG $\epsilon = 4 - d$ expansion. As shown in section 1.2, the chirality is a pseudoscalar in the *XY* case and an axial vector in the Heisenberg case. In accord with the LGW Hamiltonian (2.4), one can also generalize the definition of the chirality for general n-component spins as a second-rank antisymmetric tensor variable defined by $\kappa_{\lambda,\nu} = a_\lambda b_\mu - a_\mu b_\lambda$ $(1 \leqslant \lambda, \mu \leqslant n)$, which has $n(n-1)/2$ independent components [23].

One may define a conjugate chiral field, h_κ, which couples to a component of the chirality via a term $-h_\kappa \kappa_{\lambda,\nu}$ in the LGW Hamiltonian. Application of the chiral field h_κ reduces the original symmetry of the Hamiltonian. The non-collinear structure is then confined to the (λ, μ) plane and one of the two senses of the helix is selected. It is thus thought that the application of h_κ causes a crossover from the fully chiral behaviour to the standard *XY* behaviour.

If there is a stable fixed for $h_\kappa = 0$—say, a chiral fixed point—this crossover is governed by the chiral crossover exponent ϕ_κ associated with that fixed point. The singular part of the free energy then has a scaling form [23]

$$f_{sing} \approx F\left(\frac{h}{t^\Delta}, \frac{h_\kappa}{t^{\phi_\kappa}}\right) \tag{4.6}$$

where h is an ordering field conjugate to the order parameter $\boldsymbol{a}$ or $\boldsymbol{b}$, $\Delta \equiv \beta + \gamma$ is the gap exponent (the crossover exponent associated with the ordering field) and $t \equiv |(T - T_c)/T_c|$. If the total chirality, $\bar{\kappa} = -(\partial f/\partial h_\kappa)_{h_\kappa = 0}$, and the chiral susceptibility, $\chi_\kappa = -(\partial^2 f/\partial h_\kappa^2)_{h_\kappa = 0}$, are characterized by critical exponents β_κ and γ_κ, the above scaling gives $\beta_\kappa = 2 - \alpha - \phi_\kappa$ and $\gamma_\kappa = 2\phi_\kappa - (2 - \alpha)$, and the chirality exponents satisfy the relation

$$\alpha + 2\beta_\kappa + \gamma_\kappa = 2 \tag{4.7}$$

together with the standard relation $\alpha + 2\beta + \gamma = 2$.

In particular, in the region $n > n_{\mathrm{I}}(d)$ where the chiral fixed point is stable, the chiral crossover exponent ϕ_κ has been calculated by means of the $\epsilon = 4 - d$ expansion as [23]

$$\phi_\kappa = 1 + \frac{n^3 + 4n^2 + 56n - 96 + (n^2 - 24)\sqrt{n^2 - 24n + 48}}{4(n^3 + 4n^2 - 24n + 144)}\epsilon + O(\epsilon^2). \tag{4.8}$$

Chirality, as defined here, is a quantity *quadratic* in spin variables. At the standard $O(n)$ Wilson–Fisher fixed point, there is only *one* crossover exponent at quartic order in the spins, namely, the standard anisotropy-crossover exponent. At the $O(n)$ chiral fixed point, as a reflection of richer underlying symmetry, there generally exist *four* different crossover exponents even at the quadratic level, which physically represent *chirality*, *wavevector-dependent anisotropy*, *uniform anisotropy and wavevector-dependent energy* perturbations [23]. Among them, the chiral crossover exponent ϕ_κ is the largest. In the particular case of *XY* $(n = 2)$ spins, the discrete symmetry of the LGW Hamiltonian discussed in section 3.2 (the symmetry (iii)) mixes the two otherwise independent composite operators, uniform anisotropy and wavevector-dependent energy, and reduces this number from four to *three* [66].

4.2.3. Effects of commensurability. Under certain circumstances, the LGW Hamiltonian (2.4) could have terms with a lower symmetry. An example may be seen in the 90° spiral in helimagnets, where the turn angle is just equal to 90°. In such a case, as first noticed by Garel and Pfeuty [5], the LGW Hamiltonian has an additional quartic term of the form

$$w(\boldsymbol{a}^4 + \boldsymbol{b}^4). \tag{4.9}$$

Garel and Pfeuty studied the relevance of this quartic term by means of $\epsilon = 4 - d$ expansion, and concluded that this term was relevant in the physical case ($d = 3$, $n = 2$) and changed the nature of the helical transition from continuous to first order [5]. In contrast, the present author argued that this term was irrelevant in the ($d = 3$, $n = 2$) helical transition and that even the 90° spiral exhibited a continuous transition of $n = 2$ chiral universality [45]. The difference arises from the fact that the fixed points identified in the two cases were in fact different: the fixed point invoked by Garel and Pfeuty was the Bak and Mukamel fixed point [4] while the one invoked by the present author was the chiral fixed point [23].

4.3. $1/n$ *expansion*

In the many-component limit $n \to \infty$, the LGW Hamiltonian (2.4) can be solved exactly for arbitrary dimensionality d. In the non-collinear case $v > 0$, on which we shall concentrate in this subsection, one has a continuous transition characterized by the standard spherical-model exponents, $\alpha = (d-4)/(d-2), \beta = 1/2, \gamma = 2\nu = 2/(d-2)$ for $2 < d < 4$ [23]. (In the sinusoidal case $v < 0$, the $n \to \infty$ behaviour is more complex; see reference [67] for details.) Thus, in the non-collinear case, one can make the standard $1/n$ expansion from the spherical model based on the LGW Hamiltonian (2.4). In the $1/n$ expansion, the transition is always continuous for $2 < d < 4$: the first-order transition found in the $\epsilon = 4 - d$ expansion for $n < n_1(d)$ does not arise. Various exponents to leading order in $1/n$ were calculated as [23]

$$\gamma = \frac{2}{d-2}\left\{1 - 9\frac{S_d}{n}\right\} + \mathrm{O}\left(\frac{1}{n^2}\right) \tag{4.10}$$

$$\nu = \frac{1}{d-2}\left\{1 - 12\frac{d-1}{d}\frac{S_d}{n}\right\} + \mathrm{O}\left(\frac{1}{n^2}\right) \tag{4.11}$$

etc, where S_d is defined by

$$S_d = \sin\{\pi(d-2)/2\}\Gamma(d-1)/[2\pi\{\Gamma(d/2)\}^2]. \tag{4.12}$$

For $n \to \infty$ and $\epsilon \to 0$, these results from $1/n$ expansion match the ones from ϵ-expansion *obtained at the chiral fixed point*. On comparison with the results for the standard O(n) Heisenberg exponents, one sees that both γ and ν for the non-collinear transition are smaller than those for the collinear transition, a tendency consistent with the results of the $\epsilon = 4 - d$ expansion.

The chiral crossover exponent ϕ_κ was calculated as [23]

$$\phi_\kappa = \frac{1}{d-2}\left\{1 - 12\frac{d-1}{d}\frac{S_d}{n}\right\} + \mathrm{O}\left(\frac{1}{n^2}\right). \tag{4.13}$$

Comparison with the expression for γ shows that the chiral crossover exponent exceeds the susceptibility exponent γ, although it is smaller than the gap exponent Δ. Note that the same inequality is also satisfied within the $\epsilon = 4 - d$ expansion at the chiral fixed point. This inequality is somewhat unusual since in usual cases crossover exponents have satisfied the inequality $\phi \leqslant \gamma$. The complete spectrum of crossover exponents at the quadratic level of spins was given in reference [23].

A modified version of the $1/n$ expansion called the self-consistent screening approximation, in which the standard $1/n$ expansion is extended to smaller values of n in a self-consistent manner, was formulated by Jolicoeur [68]. A continuous transition characterized by exponents different from the standard O(n) exponents was also found, supporting the existence of a chiral universality class.

4.4. What happens in the physically relevant cases where $d = 3$ and $n = 2$ or 3?

Now, in view of the results obtained from the $\epsilon = 4 - d$ and $1/n$ expansions presented in the previous subsections, I wish to consider the physically relevant situation, where $d = 3$ and $n = 2$ or 3. The implication of the $1/n$ expansion or its extended version is simple: a new type of continuous transition characterized by exponents different from the standard O(n) exponents is suggested [23, 68]. The implications of the $\epsilon = 4 - d$ expansion are more subtle, as was summarized in figure 8. In the regime where

$$n > n_{\mathrm{I}}(d) = 21.8 - 23.4\epsilon^2 + 7.1\epsilon^3$$

there occurs a continuous transition governed by a new chiral fixed point. By contrast, for

$$n_{\mathrm{I}}(d) > n > n_{\mathrm{III}}(d) = 2 - \epsilon + 1.3\epsilon^2$$

there is no stable fixed point in the non-collinear region and the transition is expected to be first order. Finally, for $n < n_{\mathrm{III}}(d)$, the transition is governed by the standard O($2n$) Heisenberg fixed point.

At $d = 3$ and $n = 2$ or 3, this last possibility, i.e., the non-collinear transition governed by the O($2n$) Heisenberg fixed point, might be excluded, partly because all RG calculations agree that the borderline value $n_{\mathrm{III}}(d)$ lies below $n = 2$ [23, 61, 63], but also because such O($2n$) Heisenberg behaviour has not been seen in extensive Monte Carlo simulations performed on the stacked-triangular antiferromagnets [21, 33–37] (Monte Carlo results will be reviewed in the next section).

4.4.1. Continuous versus first order. Thus, the remaining question is that of whether the transition is continuous, governed by the chiral fixed point, or is first order. Of course, one can also imagine the borderline situation, i.e., the 'tricritical' case. Possible tricritical behaviour will be discussed separately in the next subsection. Answering the above question is equivalent to determining the fate of the boundary, $n_{\mathrm{I}}(d)$, at $d = 3$. As mentioned above, previous authors gave different opinions on this point. In reference [23] the present author conjectured that $n_{\mathrm{I}}(3) \leqslant 2$ by invoking Monte Carlo results. Antonenko, Sokolov and Varnashev claimed that the transition was first order on the basis of their Borel–Padé estimate, $n_{\mathrm{I}}(3) \sim 3.39$, which was slightly larger than the physical value, $n = 3$ [61]. The series for $n_{\mathrm{I}}(d)$ used in the resummation procedure, however, has only three terms, and as we have seen in the previous subsection for the *XY* sinusoidal case, it is sometimes dangerous to draw a definite conclusion on the basis of such a short series. At present, it would be fair to say that no definite conclusion could be drawn from the ϵ-expansion. Naively, one may feel that the borderline value of n_{I} at the lowest order, $n_{\mathrm{I}}(0) \simeq 21.8$, is large enough compared with the physical values $n = 2$ or 3 that one may safely conclude that the transition in real systems is first order. However, the coefficient of the first correction term, 23.4, is also large, which sets the scale of the numerics in this problem. For example, the difference between the Borel–Padé estimate of reference [61] $n_{\mathrm{I}} \simeq 3.3$ and the physical value $n = 3$ is so small compared with this scale that one can hardly hope to get a reliable answer, especially without knowledge of the asymptotic behaviour of the series.

In this connection, it might be instructive to point out that an apparently similar situation exists with respect to the phase transition of lattice superconductors (the U(1) lattice gauge model) with an n-component order parameter, where the real system corresponds to $n = 2$ [68]. A RG $\epsilon = 4 - d$ expansion calculation applied to this model yielded a stable fixed point only for very large $n > 183$, below which there was no stable fixed point [69]. Since this borderline value of $n \sim 183$ was so large compared with the physical value $n = 2$, it was initially concluded that the normal–superconducting transition of charged superconductors should be first order [69]. However, it is now well established through duality analysis and Monte Carlo simulation that the $n = 2$ superconductor in fact shows a continuous transition of the inverted-XY type [70, 71]. So, the low-order $\epsilon = 4 - d$ expansion clearly gives a wrong answer in this case. By contrast, $1/n$ expansion and its modified version (the self-consistent screening approximation) correctly yielded a continuous transition [69, 72].

Presumably, the only way in which one could get a more or less reliable answer from the RG loop expansion is to obtain the large-order behaviour of the series (the large-order perturbation), possibly with a few more terms in the expansion [73]. We leave such a calculation applied to the non-collinear transition to future studies.

It might also be important to point out here that, even when a stable fixed point exists as in regime I, a first-order transition is still possible, depending on the microscopic parameters of the system. This is simply due to the fact that even in the type of RG flow diagram shown in figure 7(a) the flow could show a runaway only if the initial point representing a particular microscopic system is located *outside* the domain of attraction of the stable fixed point. This means that, even if one has a few non-collinear systems exhibiting a first-order transition, it does not necessarily exclude the possibility of a group of other non-collinear magnets showing a continuous transition. The difference between these two types of system is not of symmetry origin, but arises simply from the difference in certain non-universal parameters.

One might then hope to get information about the location of the initial point of the RG flows in the parameter space, by mapping the original microscopic spin Hamiltonian into the LGW form. Of course, there usually remain some ambiguities in the procedure because such a mapping also generates higher-order irrelevant terms in the LGW Hamiltonian (various terms higher than sixth order in $\boldsymbol{a}$ and $\boldsymbol{b}$), which modifies the initial values of the quartic terms u and v somewhat through a few initial RG iterations. Anyway, such a mapping performed in reference [23] shows that in both cases of stacked-triangular antiferromagnets and helimagnets one has $v_0/u_0 = 4/3$, where u_0 and v_0 are the initial values of quartic coupling constants. In a situation where the chiral fixed point exists at all, this point is likely to lie *inside* the domain of the fixed point. Indeed, the ratio v/u at the chiral fixed point in the borderline case $n = n_{\mathrm{I}}$ is estimated from the $\epsilon = 4-d$ expansion as $v_0/u_0 = 3.11+\mathrm{O}(\epsilon)$.

By contrast, there are several models with the same chiral symmetry whose initial point of the RG flow lies outside the domain of attraction of the chiral fixed point. An example is the matrix O(2) model describing $n = 2$ non-collinear magnets, in which the non-collinear structure is completely rigid. In this model, the above mapping yields the initial point at $v_0/u_0 = 4$ [74], which is expected to lie *outside* the domain of attraction of the chiral fixed point. Here, recall that the line $v/u = 4$ corresponds to the stability boundary in the mean-field approximation as shown in section 4.1, and is likely to lie outside the domain of attraction of any stable fixed point. In fact, a first-order transition was observed for the matrix O(2) model in $d = 3$ dimensions by Monte Carlo simulation [75], consistently with the above argument. In the $\mathrm{O}(3)_L \times \mathrm{O}(2)_R$ matrix model representing the completely rigid $n = 3$ non-collinear magnets, the above mapping yields $v_0/u_0 = 3$ [74]. For this matrix model in $d = 3$ dimensions, Kunz and Zumbach observed by means of

Monte Carlo simulation a continuous transition with the unusual critical exponent $\nu \sim 0.48$ [75]. For the stacked-triangular Heisenberg antiferromagnet, Dobry and Diep observed by means of Monte Carlo simulation that, if one stiffened the non-collinear 120° structure by adjusting some of the exchange constants, the nature of the transition apparently changed significantly [76]. This observation might also be understandable within the above picture, if one considers the initial point of the RG flow moving in the parameter space toward a runaway region as the non-collinear 120° spin structure is stiffened.

Since there appears to be a possibility that $n_{\rm I}(d = 3)$ lies close to the physical values $n = 2$ or 3, it may be interesting to examine what happens if $n_{\rm I}(3)$ is only very slightly larger than the physical value of n. In this case, although there is no stable fixed point in the strict sense (the chiral fixed point becomes complex valued in this regime), RG flows behave as if there were a stable fixed point for a long period of iterations. Thus, as illustrated in figure 9, a 'shadow' of the chiral fixed point attracts the RG flows up to a certain scale, but, eventually, the flow escapes away from such a 'pseudo-fixed point' through a narrow channel in the parameter space and shows a runaway signalling a first-order transition. Physically, this means that the system exhibits a rather well-defined critical behaviour for a wide range of temperature governed by the complex-valued chiral fixed point, but eventually, the deviation from such critical behaviour sets in for sufficiently small t, and the system exhibits a weak first-order transition. This scenario is perhaps close to the 'almost continuous transition' scenario proposed by Zumbach [77, 78]. It was suggested there within the local potential approximation of the RG that the transition of $n = 3$ non-collinear magnets might be almost continuous with well-defined pseudo-critical exponents.

4.4.2. Possible tricritical behaviours. A few authors have suggested that the $d = 3$ non-collinear transition might be tricritical. More specifically, *mean-field* tricritical behaviour was invoked in those studies [31, 32, 36]. It should be noticed, however, that the tricriticality in general is not necessarily mean-field tricritical, particular when the LGW Hamiltonian has more than one quartic coupling as in our model [79]. In this subsection, I will examine the

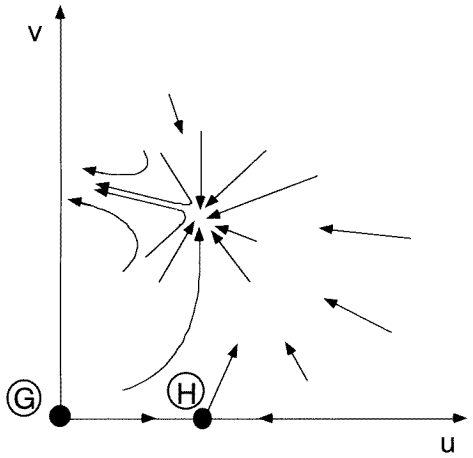

Figure 9. Renormalization-group flows in the (u, v) plane in the non-collinear region $v > 0$, expected when n is only slightly smaller than $n_{\rm I}(d)$. There remains a 'shadow' of the slightly complex-valued chiral fixed point which attracts the flows up to a certain scale. Eventually, all flows show runaway, signalling a weak first-order transition.

possible tricritical behaviours in the non-collinear transition based on the LGW Hamiltonian (2.4) and the picture derived from $\epsilon = 4 - d$ expansion. Since the word 'tricritical' has sometimes been used in the literature in a rather wide or vague sense, I will try to be unambiguous here as regards what is meant by tricriticality. The two different 'tricritical' cases will be discussed.

The standard tricritical situation is concerned with a separatrix of the RG flows which divides the two regions of the parameter space, one associated with a continuous transition and the other with a first-order transition. In the case where the chiral fixed point is stable, this separatrix is the line connecting the Gaussian fixed point G and the antichiral fixed point C_-, the latter being the tricritical fixed point; see figure 7(a). By its definition, the tricritical fixed point has one more relevant operator in addition to the temperature and the ordering field. Thus, if the initial Hamiltonian happens to lie at a point on this separatrix, the RG flow is attracted to the tricritical fixed point C_- and the system exhibits a tricritical behaviour governed by the antichiral fixed point C_-. In order to reach this tricritical fixed point, one has to tune one symmetry-unrelated microscopic parameter in such a way that the initial point is just on the separatrix. Since the tricritical fixed point here is not the Gaussian fixed point G, but the non-trivial antichiral fixed point C_-, the associated tricritical exponents are *not* mean-field tricritical. As usual, a change in a certain non-universal parameter of the system would induce either a first-order transition or a continuous transition governed by the stable chiral fixed point C_+.

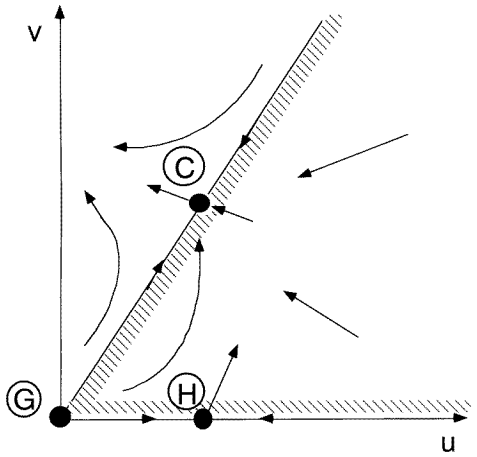

Figure 10. Renormalization-group flows in the (u, v) plane in the non-collinear region $v > 0$ just at $n = n_1(d)$. The hatched regions represent basins of attraction of the stable fixed point. The fixed point C is doubly degenerate, C_+ and C_-. It is a non-trivial fixed point with a finite domain of attraction in the (u, v) plane.

The second 'tricritical' case is concerned with the situation where the physical value of n is just at the borderline value $n = n_1(d)$ between the regimes of continuous and first-order transitions. In this case, the RG flow diagram becomes as given in figure 10, where the two fixed points C_+ and C_- coalesce at a point in the (u, v) plane. As can be seen in figure 10, the resulting fixed point, which is again a highly non-trivial one, has a finite domain of attraction in the (u, v) plane and attracts many microscopic Hamiltonians, in contrast to the tricritical fixed point discussed above. Therefore, except for the degenerate nature of the fixed point, the situation is essentially the same as in the case of $n > n_1(d)$, in the sense

that novel critical behaviour is expected for a variety of microscopic systems.

Note that, in both of the cases discussed above, the tricritical behaviour is highly non-trivial, *not mean-field tricritical*. This is simply due to the fact that the tricritical fixed point is a non-trivial one reflecting the existence of more than one quartic coupling constant in the LGW Hamiltonian. Of course, the Gaussian fixed point responsible for the mean-field tricritical behaviour always exists at the origin, but, to reach this fixed point, one has to tune more than one symmetry-unrelated microscopic parameter, and the occurrence of such a mean-field tricritical transition is highly unlikely [79].

4.5. $\epsilon = d - 2$ expansion

In this subsection, I will review an alternative RG approach, an expansion from the lower critical dimension $d_< = 2$. This method was first applied to the non-collinear transition by Azaria, Delamotte and Jolicoeur for the Heisenberg spins ($n = 3$) [31]. Extension to general n-component spins was made by Azaria, Delamotte, Delduc and Jolicoeur [32], and by the present author [80].

4.5.1. The non-linear sigma model. In contrast to the $\epsilon = 4 - d$ expansion, the $\epsilon = d - 2$ expansion is based on the non-linear sigma model which is written in terms of spin variables of fixed length. In the case of non-collinear magnets with n-component spins, this may be written in terms of two mutually orthogonal n-component vector fields $\boldsymbol{a}$ and $\boldsymbol{b}$ as

$$\mathcal{H} = \frac{1}{2T}\left[(\nabla_\mu \boldsymbol{a})^2 + (\nabla_\mu \boldsymbol{b})^2 + r \sum_{1 \leqslant i < j \leqslant n} \{\nabla_\mu (a_i b_j - a_j b_i)\}^2\right] \tag{4.14a}$$

with the constraints

$$|\boldsymbol{a}(\boldsymbol{r})| = |\boldsymbol{b}(\boldsymbol{r})| = 1 \qquad \boldsymbol{a}(\boldsymbol{r}) \cdot \boldsymbol{b}(\boldsymbol{r}) = 0 \tag{4.14b}$$

where T is a temperature and r is a coupling-constant ratio. One can easily check that the above Hamiltonian satisfies the same $\mathrm{O}(n) \times \mathrm{O}(2)$ symmetry as the LGW Hamiltonian (2.4). Unlike the case of equation (2.4), the non-collinear structure, i.e., an orthogonal frame spanned by the two vectors $\boldsymbol{a}$ and $\boldsymbol{b}$, is completely rigid here. It is not necessarily obvious whether this idealization changes the essential physics in $d = 3$ dimensions (recall our discussion concerning the stiffness of the non-collinear structure in the previous subsection based on the LGW Hamiltonian).

4.5.2. Fixed points and exponents. The standard $\epsilon = d - 2$ expansion applied to the Hamiltonian (4.14) yields a stable fixed point characterized by the exponents [32, 80]

$$\nu = \epsilon - \frac{1}{2}\frac{6n^3 - 27n^2 + 32n - 12}{(n-2)^3(2n-3)}\epsilon^2 + \mathrm{O}(\epsilon^3) \tag{4.15}$$

$$\eta = \frac{3n^2 - 10n + 9}{2(n-2)^3}\epsilon + \mathrm{O}(\epsilon^2). \tag{4.16}$$

This fixed point is stable for any $n > 2$ and $d > 2$. In the limit $n \to 2$, the fixed-point temperature tends to infinity and the $\epsilon = d - 2$ expansion becomes meaningless. Azaria *et al* observed that, in the particular case of Heisenberg spins ($n = 3$), the fixed point obtained was nothing but the standard O(4) Wilson–Fisher fixed point [31]. Note that this O(4) fixed point is different in nature from the O(4)-like fixed point obtained by Bak and Mukamel in the $\epsilon = 4 - d$ expansion analysis of the XY ($n = 2$) non-collinear magnets: the former

fixed point has no counterpart in the $\epsilon = 4 - d$ expansion [4]. By contrast, for $n > 3$, the fixed point obtained by means of the $\epsilon = d - 2$ expansion is a new one, *not* the standard Wilson–Fisher fixed point. Indeed, for large enough n, various exponents reduce to those obtained by means of the $1/n$ expansion based on the LGW Hamiltonian [23], naturally fitting into the chiral-fixed-point picture obtained via the $\epsilon = 4 - d$ and $1/n$ expansions.

As already mentioned, in the Heisenberg ($n = 3$) case, $\epsilon = d - 2$ expansion predicts that the symmetry is dynamically restored, yielding the standard O(4) critical behaviour which has never been seen in the $\epsilon = 4 - d$ expansion. On the basis of this observation, Azaria *et al* claimed that the ($n = 3$, $d = 3$) non-collinear transition should be of standard O(4) universality [31, 32]. They further speculated that the transition could also be first order or mean-field tricritical, depending on the microscopic parameters of the system. (Note, however, that the $\epsilon = d - 2$ expansion itself yielded neither first-order nor mean-field tricritical behaviour.) So, in the 'non-universality' scenario of reference [31], the non-collinear transition of Heisenberg systems is either O(4), mean-field tricritical, or first order.

4.5.3. Discussion. In fact, as will be shown in the next section, recent extensive Monte Carlo simulations on the stacked-triangular Heisenberg antiferromagnets now rule out the possibility of O(4)-like critical behaviour [31, 33, 35, 37]. Thus, doubt has been cast by several authors on the validity of the $\epsilon = d - 2$ method applied to this problem. In the Heisenberg case ($n = 3$), a different interpretation of the O(4) behaviour obtained by means of the $\epsilon = d - 2$ expansion had already been given in reference [80]: it was argued there that the O(4) fixed point for $n = 3$ was spurious, arising from the inability of the method to deal with the crucially important non-perturbative effects associated with the vortex degrees of freedom, which reflects the non-trivial topological structure of the order-parameter space, $\Pi_1(V = \mathrm{SO}(3)) = \mathrm{Z}_2$. Essentially the same criticism was also made by Kunz and Zumbach, and by Zumbach in references [75] and [81].

By analysing the properties of another generalization of the $n = 3$ model, the $\mathrm{O}(n) \times \mathrm{O}(n-1)$ non-linear sigma model, David and Jolicoeur proposed a scenario in which Azaria's O(4) fixed point with enlarged symmetry played no role due to the appearance of a first-order line in the phase diagram [82]. (Note that the 'principal chiral fixed point' quoted by these authors corresponds to the O(4) fixed point with enlarged symmetry, *not* the chiral fixed point in the present article.) On the other hand, on the basis of their Monte Carlo study of a modified stacked-triangular Heisenberg antiferromagnet in which the interaction is modified to yield the rigid 120° structure, Dobry and Diep suggested that the non-linear sigma model used by Azaria *et al* itself might already be inappropriate for modelling the original stacked-triangular Heisenberg antiferromagnet [76].

While the above criticisms apply specifically to the $n = 3$ non-collinear magnets, it should also be mentioned that there has been controversy concerning the validity of the $\epsilon = d - 2$ expansion method even in the simplest case of simple $\mathrm{O}(n)$ ferromagnets [83]. Anyway, it now appears clear for the present problem that the $\epsilon = d - 2$ expansion method is problematic, at least in the case of $n = 3$. Special care has to be taken in applying this method to the system with non-trivial internal structure in its order-parameter space, like the non-collinear magnets.

4.6. Further generalization of non-collinear transitions

So far, we have limited our discussion to the magnets with non-collinear but *coplanar* spin order. On the other hand, in some cases, *non-coplanar* spin orderings that are three

dimensional in spin space could appear. An example is a triple-$\boldsymbol{Q}$ ordering as illustrated in figure 11. One can further generalize the situation to m-dimensional spin order in isotropic n-spin space with $m \leqslant n$. The $m = 1$ case represents the collinear spin order, while the $m = 2$ case represents the non-collinear but coplanar spin order discussed so far. Then, one can naturally imagine the possible existence of hyperuniversality series characterized by two integers (m, n).

Theoretical analysis of such non-coplanar criticality was first carried out in 1990 by the present author on the basis of a symmetry argument, and RG $\epsilon = 4-d$ and $1/n$ expansions [84]. An appropriate LGW Hamiltonian with the $\mathrm{O}(m) \times \mathrm{O}(n)$ symmetry is given by

$$\mathcal{H}_{\mathrm{LGW}} = \frac{1}{2}\sum_{\alpha}(\nabla\phi_\alpha)^2 + \frac{1}{2}r\sum_{\alpha}\phi_\alpha^2 + \frac{1}{4!}u\left(\sum_{\alpha}\phi_\alpha^2\right)^2 + \frac{1}{4!}v\sum_{\langle\alpha\beta\rangle}\{(\phi_\alpha\cdot\phi_\beta)^2 - \phi_\alpha^2\phi_\beta^2\} \tag{4.17}$$

where the ϕ_α $(1 \leqslant \alpha \leqslant m)$ are m sets of n-component vectors. The condition

$$0 < v < \frac{2m}{m-1}u \tag{4.18}$$

is required by the non-coplanarity of the ordering and the boundedness of the free energy. The $\epsilon = 4 - d$ expansion applied to (4.17) yields a generalized chiral fixed point in the non-collinear region $v > 0$, which is stable for [84]

$$n > n_{\mathrm{I}}(d) = 5m + 2 + 2\sqrt{6(m+2)(m-1)} - \left\{5m + 2 + \frac{25m^2 + 22m - 32}{2\sqrt{6(m+2)(m-1)}}\right\}\epsilon + \mathrm{O}(\epsilon^2). \tag{4.19}$$

For the coplanar ($m = 2$) case, this reduces to the previous result (4.3), while in the non-coplanar ($m = 3$) case, this gives

$$n > n_c(d) = 32.5 - 33.7\epsilon + \mathrm{O}(\epsilon^2). \tag{4.20}$$

Again, it is not easy to tell from this expression whether the non-coplanar ($m = 3$) chiral fixed point remains stable in the physical case, where $d = 3$ and $n = 3$.

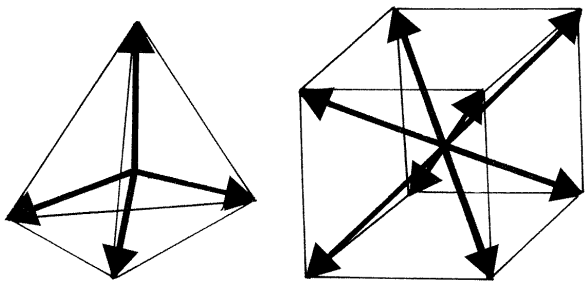

Figure 11. An illustration of non-coplanar spin orderings like the ones realized in triple-$\boldsymbol{Q}$ structures in type-I (left) and in type-II (right) fcc antiferromagnets.

The exponents γ and ν at this generalized chiral fixed point were calculated as [84]

$$\begin{aligned}
&\gamma \approx 2\nu = 1 + \frac{1}{4} B_{mn}(C_{mn} + D_{mn}\sqrt{R_{mn}})\epsilon + \mathrm{O}(\epsilon^2) \\
&B_{mn}^{-1} = (mn+8)(m+n-8)^2 + 24(m-1)(n-1)(m+n-2) \\
&C_{mn} = mn(m+n)^2 + 8mn(m+n) - 22(m+n)^2 + 88mn - 32(m+n) + 152 \\
&D_{mn} = mn(m+n) - 10(m+n) + 4mn - 4 \\
&R_{mn} = (m+n-8)^2 - 12(m-1)(n-1).
\end{aligned} \tag{4.21}$$

The $1/n$ expansion applied to (4.17) yields a continuous transition characterized by the exponents [84]

$$\gamma = \frac{2}{d-2}\left\{1 - 3(m+1)\frac{S_d}{n}\right\} + \mathrm{O}\left(\frac{1}{n^2}\right) \tag{4.22}$$

$$\nu = \frac{1}{d-2}\left\{1 - 4(m+1)\frac{d-1}{d}\frac{S_d}{n}\right\} + \mathrm{O}\left(\frac{1}{n^2}\right) \tag{4.23}$$

where S_d was defined by (4.12). Further details including the expression for the chiral crossover exponent were given in reference [84]. (Some of the $\epsilon = 4 - d$ expansion results at the lowest order were also reported in reference [85], in apparent ignorance of reference [84].) Anyway, if this generalized chiral fixed point remains stable for $d = 3$, the associated critical behaviour is most probably novel. Thus, the possible existence of a hyperseries of universality classes characterized by two integers m and n was proposed in reference [84], where the special case with $m = 1$ corresponds to the standard O(n) Wilson–Fisher universality and the case with $m = 2$ corresponds to the standard chiral universality.

One possible example of such non-coplanar criticality was studied by Reimers, Greedan and Björgvinsson for the pyrochlore antiferromagnet FeF_3 both by means of a neutron diffraction experiment and by Monte Carlo simulation [86]. The reported exponent values were quite unusual, $\alpha = 0.6(1), \beta = 0.18(2), \gamma = 1.1(1)$ and $\nu = 0.38(2)$, although Mailhot and Plumer argued that the same data were also not inconsistent with a first-order transition [87].

5. Monte Carlo simulations

5.1. Stacked-triangular antiferromagnets

In this section, I wish to review the results of Monte Carlo simulations for the 3D *XY* and Heisenberg antiferromagnets on a stacked-triangular lattice. The Monte Carlo method enables us to study the *XY* and Heisenberg systems directly in three dimensions. Thus, if one could control finite-size effects and statistical errors intrinsic to the method, one could get useful information which might serve to test various theoretical proposals.

Partly for simplicity and partly to get a wide critical regime, most of the extensive Monte Carlo simulations on the stacked-triangular antiferromagnets were performed on the nearest-neighbour Hamiltonian (2.1) with $J = J'$. Earlier work by the present author simulated lattices up to $L = 60^3$ both for *XY* and Heisenberg models on the basis of the conventional method [21], while more recent simulations on the *XY* model by Plumer and Mailhot [36], by Boubcheur, Loison and Diep [34], and those on the Heisenberg model by Bhattacharya, Billoire, Lacaze and Jolicoeur [33], by Mailhot, Plumer and Caillé [37], and by Loison and Diep [35] used the histogram technique, the largest lattice sizes being $L = 33$–48. As an

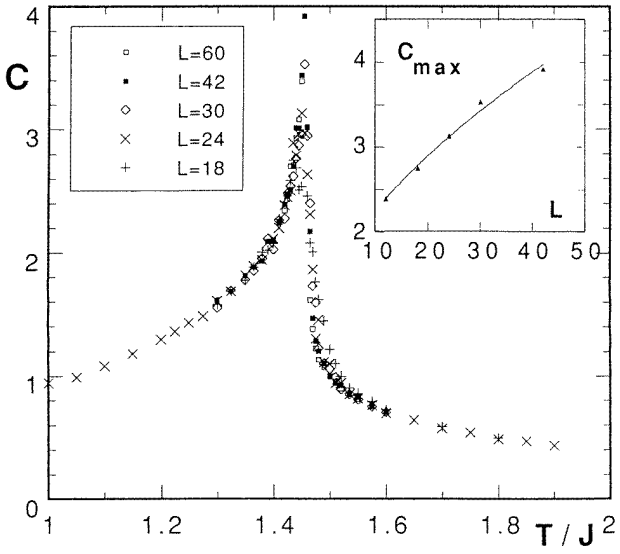

(a)

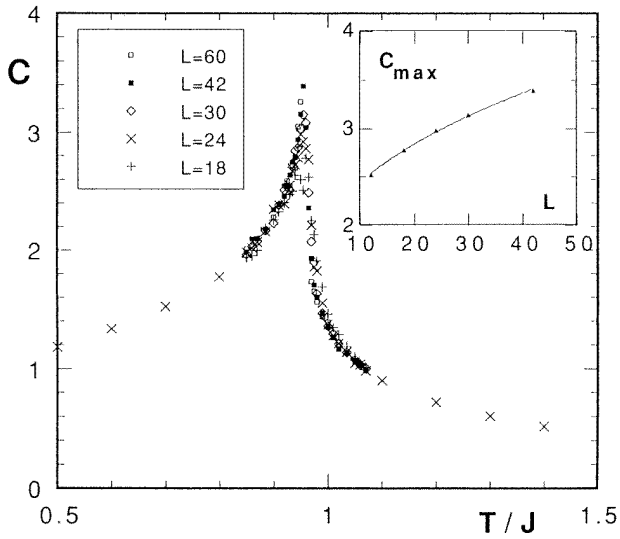

(b)

Figure 12. The temperature and size dependence of the specific heat calculated by Monte Carlo simulation of the stacked-triangular (a) *XY* and (b) Heisenberg antiferromagnets with L^3 spins. The data are taken from reference [21]. The insets exhibit the size dependence of the specific-heat peak.

example, the temperature and size dependence of the specific heat calculated in reference [21] is reproduced in figure 12. In the numerical sense, the results obtained by these independent simulations agreed with each other except for a small deviation remaining in some exponents in the *XY* case. In all such studies a continuous transition was observed for both the *XY* and the Heisenberg cases, except in the recent simulation by Plumer and Mailhot on a *quasi-one-dimensional* stacked-triangular *XY* antiferromagnet [88].

Table 2. Critical exponents, amplitude ratios and transition temperatures as determined by several Monte Carlo simulations for the stacked-triangular XY antiferromagnet with $J = J'$. The maximum lattice size used in each simulation is also shown. The corresponding values of the standard XY, O(4) and mean-field tricritical universality classes are also shown.

	Kawamura [21]	Plumer and Mailhot [36]	Boubcheur *et al* [34]	XY	O(4)	Mean-field tricritical
Maximum size	60^3	33^3	42^3			
T_c/J	1.458(2)	1.4584(6)	1.4580(5)			
α	0.34(6)	0.46(10)	0.46(10)	−0.008	−0.22	0.5
β	0.253(10)	0.24(2)	0.25(2)	0.35	0.39	0.25
γ	1.13(5)	1.03(4)	1.15(5)	1.316	1.47	1
ν	0.54(2)	0.50(1)	0.48(2)	0.669	0.74	0.5
A^+/A^-	0.36(20)	—	—	0.99	—	0
β_κ	0.45(2)	0.38(2)	—	—	—	
γ_κ	0.77(5)	0.90(9)	—	—	—	
ν_κ	0.55(2)	0.55(1)	—	—	—	

Table 3. Critical exponents, amplitude ratios and transition temperatures as determined by several Monte Carlo simulations for the stacked-triangular Heisenberg antiferromagnet with $J = J'$. The maximum lattice size used in each simulation is also shown. The corresponding values of the standard Heisenberg, O(4) and mean-field tricritical universality classes are also shown.

	Kawamura [21]	Bhattacharya *et al* [33]	Mailhot *et al* [37]	Loison and Diep [35]	Heisenberg	O(4)	Mean-field tricritical
Maximum size	60^3	$48^2 \times 32$	36^3	36^3			
T_c/J	0.958(4)	0.9576(2)	0.9577(2)	—			
α	0.24(8)	—	—	—	−0.116	−0.22	0.5
β	0.30(2)	0.289(10)	0.285(11)	0.28(2)	0.36	0.39	0.25
γ	1.17(7)	1.176(20)	1.185(3)	1.25(3)	1.387	1.47	1
ν	0.59(20)	0.585(9)	0.586(8)	0.59(1)	0.705	0.74	0.5
A^+/A^-	0.54(20)	—	—	—	1.36	—	0
β_κ	0.55(4)	—	0.50(2)	—	—	—	0.5
γ_κ	0.72(8)	—	0.82(4)	—	—	—	0.5
ν_κ	0.60(3)	—	0.608(12)	—	—	—	0.5

The values of the critical exponents, specific-heat amplitude ratios and transition temperatures reported by these authors are summarized in tables 2 and 3 for both cases of XY and Heisenberg models, and are compared with the corresponding values for unfrustrated XY and Heisenberg ferromagnets, for the standard O(4) behaviour and for the mean-field tricritical behaviour. One can immediately see that the exponent values determined by these simulations differ significantly from the unfrustrated XY or Heisenberg values. One can also see that the reported exponents are incompatible with the O(4) exponents in both the XY and the Heisenberg cases which were predicted by Bak and Mukamel (in the XY case) [4] and by Azaria *et al* (in the Heisenberg case) [31]. Indeed, the O(4) singularity is weaker than that of the standard XY and Heisenberg singularity, contrary to the observed tendency. On the basis of these findings, one may now rule out the standard O(4)-like critical behaviour in both cases of XY and Heisenberg magnets. In the Heisenberg case, the reported exponents are also inconsistent with the mean-field tricritical values suggested by Azaria *et al* [31], and give support to the claim that the $n = 3$ non-collinear transition

is indeed of the new $n = 3$ chiral universality.

In the *XY* case, one sees from the table that the reported exponent values are not much different from the mean-field tricritical values. Furthermore, a closer look reveals that there remain small differences between the exponent values reported by the three different groups. All agree concerning the exponent β, which comes out at around 0.25. By contrast, for the exponent γ, the reported values are scattered: 1.03 ± 0.04 (reference [36]), 1.13 ± 0.05 (reference [21]) and 1.15 ± 0.05 (reference [34]). The reason for this deviation is not clear. In fact, the exponent values reported by Plumer and Mailhot in reference [36] were very close to the mean-field tricritical values, and these authors suggested that the transition in the *XY* case might indeed be mean-field tricritical. In contrast to this, finite-size scaling analysis in reference [21] favoured the non-trivial exponents, rather than the mean-field tricritical exponents.

Meanwhile, larger deviations from the mean-field values were observed in the chirality exponents β_κ and γ_κ and the specific-heat amplitude ratio A^+/A^-. In the mean-field tricritical case governed by the Gaussian fixed point, these values should be $\beta_\kappa = 0.5$, $\gamma_\kappa = 0.5$ and $A^+/A^- = 0$, while the Monte Carlo results of reference [21] yielded $\beta_\kappa = 0.45 \pm 0.02$, $\gamma_\kappa = 0.77 \pm 0.05$ and $A^+/A^- = 0.36 \pm 0.2$ in the *XY* case, and $\beta_\kappa = 0.55 \pm 0.04$, $\gamma_\kappa = 0.72 \pm 0.08$ and $A^+/A^- = 0.54 \pm 0.2$ in the Heisenberg case. These non-trivial values of the chirality exponents and the specific-heat amplitude ratios appear to be hard to explain on the basis of the mean-field tricritical scenario. The observed chirality exponents satisfy the scaling relation (4.7) within the error bars.

In reference [36], Plumer and Mailhot suggested the possibility that the chirality and the spin are decoupled and order at slightly different temperatures, $T_c \neq T_c^{(\kappa)}$, and/or with mutually different correlation-length exponents, $\nu \neq \nu_\kappa$. From the standard theory of critical phenomena, however, this is a rather unlikely situation in the present 3D problem for the following reason. If the chirality were decoupled from the spin and exhibited an independent transition, the criticality associated with this chirality transition would be expected to be of 3D Ising universality, which should then give $\beta_\kappa \sim 0.324$, $\gamma_\kappa \sim 1.239$ and $\nu_\kappa \sim 0.629$ etc. However, this clearly contradicts the Monte Carlo results. Even if the criticality of the decoupled chirality transition were to differ from the standard Ising one for some unknown reason, the chiral susceptibility exponent γ_κ in such a case should definitely be larger than unity, which again seems hard to reconcile with the Monte Carlo results $\gamma_\kappa = 0.77 \pm 0.05$ [21] or $\gamma_\kappa = 0.90 \pm 0.09$ [36]. Rather, the Monte Carlo observation that $T_c \sim T_c^{(\kappa)}$ and $\nu \sim \nu_\kappa$, together with the non-Ising values of the chirality exponents, constitutes a clear indication that the spin and the chirality are *not* decoupled and that the chirality behaves as a composite operator of the order parameter, the spin. In fact, this is just the scenario suggested on the basis of the RG analysis in section 4.2 [23]. Note that, in such a situation, the chirality exponents are generally non-Ising and the chiral susceptibility exponent γ_κ could be less than unity, in accord with the Monte Carlo results. As long as the spin and the chirality are not decoupled at the transition, the observed non-trivial values of the chirality exponents are unambiguous indications that the transition here is *not* mean-field tricritical.

Monte Carlo simulation is performed for finite systems (in the present case, $L \leqslant 60^3$), and one cannot completely rule out the possibility that an indication of a first-order transition eventually develops for still larger lattices. Mailhot and Plumer recently performed a histogram Monte Carlo simulation of a quasi-one-dimensional stacked-triangular *XY* antiferromagnet in which the interplane interaction is much stronger than the intraplane interaction ($J' = 10J$) for lattice sizes up to $L = 33^3$, and claimed that the transition was weakly first order [88]. More specifically, these authors estimated the transition temperature

by two different methods which gave somewhat different estimates of T_c (about 0.5% difference). If a higher estimate of T_c was employed in the fit, finite-size scaling of the data was suggestive of a first-order transition, while if a lower estimate of T_c was employed, it was suggestive of a continuous transition with the exponents close to those of previous work [36]. In view of the rather large uncertainty in their estimate of T_c as well as the high sensitivity of the results to the assumed T_c-value, and also of the fact that they never observed a double-peak structure in the energy histogram characteristic of a first-order transition [88], the claimed first-order nature of the transition seems not necessarily conclusive. One should also be careful that, in highly anisotropic systems like the one studied in reference [88], there generally occurs a dimensional crossover which might complicate the data analysis particularly when the system size is not large enough.

5.2. Helimagnets

While the stacked-triangular antiferromagnets are the best-studied model, there have been a few Monte Carlo investigations of 3D helimagnets (spiral magnets). Diep simulated a helimagnetic model with competing nearest- and next-nearest-neighbour antiferromagnetic interactions on a body-centred-tetragonal lattice under periodic boundary conditions [89]. In the case of Heisenberg spins, Diep observed a continuous transition characterized by the exponents $\alpha = 0.32 \pm 0.03$ and $\nu = 0.57 \pm 0.02$, which were not far from the $n = 3$ chiral values obtained for the stacked-triangular Heisenberg antiferromagnet. In the case of *XY* spins, he observed either two successive continuous transitions or a first-order transition, depending on the microscopic parameters of the model.

One potential problem exists, however, in the simulation of helimagnets of this type. That is, unlike the 120° spin structure in the triangular antiferromagnets, the pitch of a magnetic spiral is generally *temperature dependent* and is *incommensurate* with the underlying lattice. Therefore, imposed periodic boundary conditions, even if they are chosen to accommodate the ground-state spin configuration without mismatch, generally cause a mismatch around T_c causing an artificial 'stress' on the helical spin structure. This could have a significant effect on the nature of the phase transition [90], particularly when the lattice size is not large enough compared with the spiral pitch.

5.3. Matrix models

Finally, several matrix models expected to model non-collinear magnets were also studied by Monte Carlo simulations. The Hamiltonian of these matrix models may be given by

$$\mathcal{H} = -J \sum_{\langle ij \rangle} \mathrm{Tr}(O_i^{\mathrm{T}} O_j) \tag{5.1}$$

where O_i is a matrix variable at the ith site of a simple cubic lattice and $J > 0$ is the ferromagnetic nearest-neighbour coupling. Relevant to our present study is the matrix O(2) model representing the non-collinear *XY* magnets, where the matrix variable O_i is a 2×2 orthogonal matrix, and the matrix $\mathrm{O}(3)_L \times \mathrm{O}(2)_R$ model, representing the non-collinear Heisenberg magnets, where O_i is a 3×2 matrix written in terms of two orthogonal unit three-vectors, $\boldsymbol{a}$ and $\boldsymbol{b}$, as $(\boldsymbol{a}, \boldsymbol{b})$.

In the O(2) case, the model has an $\mathrm{O}(2)_L \times \mathrm{O}(2)_R$ symmetry and is also equivalent to the coupled Ising–*XY* model of the form

$$\mathcal{H} = -J \sum_{\langle ij \rangle} (1 + \sigma_i \sigma_j) \cos(\theta_i - \theta_j) \tag{5.2}$$

where $\sigma_i = \pm 1$ is an Ising variable and $\theta_i = [0, 2\pi)$ is an angle variable of the XY spin.

As previously mentioned, these matrix models represent completely rigid non-collinear spin structures. The analysis in section 4 suggests that these models, particularly the matrix O(2) model, are likely to exhibit a first-order transition since the initial point of the associated RG flow might be located in the runaway region in the parameter space. Indeed, Monte Carlo simulations by Kunz and Zumbach [75], and by Dobry and Diep [76], based on these and related models, revealed that the 3D matrix models exhibited a first-order transition, or behaviour close to it.

As pointed out by Zumbach [78], the matrix O(2) model shows an interesting transition behaviour *even at the mean-field level*, significantly different from that of stacked-triangular antiferromagnets with non-rigid non-collinear spin structures: it exhibits a mean-field tricritical transition with the exponents $\alpha = 1/2$, $\beta = 1/4$ and $\gamma = 1$, which should be contrasted with the ordinary mean-field exponents $\alpha = 0$, $\beta = 1/2$ and $\gamma = 1$ observed when the mean-field approximation is applied to the XY and Heisenberg stacked-triangular antiferromagnets. By contrast, the $O(3)_L \times O(2)_R$ matrix model modelling the rigid Heisenberg non-collinear magnets exhibits an ordinary mean-field transition at the mean-field level [78]. These observations suggest that the nature of the transition of the matrix models or the coupled Ising–XY model may not always be the same as those of the original non-collinear magnets with non-rigid non-collinear spin structures, even when they share the same symmetry.

6. Experiments

In this section, we briefly review the recent experimental results both on (a) stacked-triangular antiferromagnets and (b) helimagnets (spiral magnets). Since some review articles with emphasis on experimental work are already available [42, 44], I summarize here some of the main features and highlight the points of interest.

Table 4. Critical exponents and amplitude ratios determined by experiments on several stacked-triangular XY antiferromagnets. The values given by several theories are also shown.

	α	β	γ	ν	A^+/A^-
$CsMnBr_3$	0.39(9) [26] 0.40(5) [27]	0.22(2) [24] 0.25(1) [25] 0.21(2) [24] 0.24(2) [39]	1.10(5) [25] 1.01(8) [24]	0.57(3) [25] 0.54(3) [24]	0.19(10) [26] 0.32(20) [27]
$CsNiCl_3$ at $H = H_m$	0.37(8) [91] 0.342(5) [92]	0.243(5) [93]	—	—	0.30(11) [91]
$CsMnI_3$ at $H = H_m$	0.34(6) [138]	—	—	—	0.31(8) [92]
XY	−0.008	0.35	1.316	0.669	0.99
$n = 2$ chiral [21]	0.34(6)	0.253(10)	1.13(5)	0.54(2)	0.36(20)
O(4)	−0.22	0.39	1.47	0.74	—
Mean-field tricritical	0.5	0.25	1.0	0.5	0

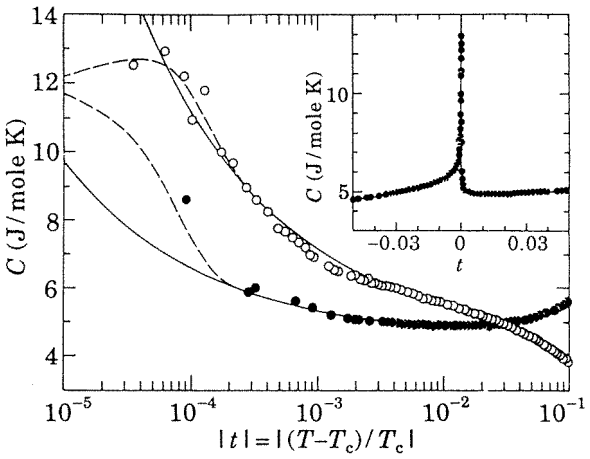

Figure 13. The specific heat versus the reduced temperature $|t|$ for the stacked-triangular *XY* antiferromagnet $CsMnBr_3$, taken from reference [27]. The inset shows the specific heat in a linear representation.

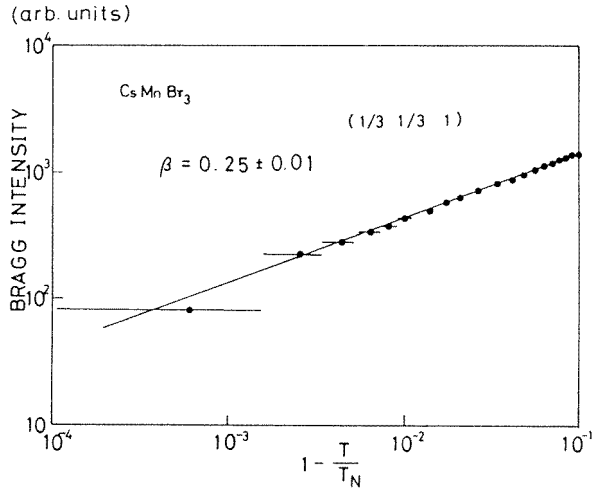

Figure 14. The magnetic Bragg intensity of the $(1/3, 1/3, 1)$ reflection measured by means of neutron diffraction for the stacked-triangular *XY* antiferromagnet $CsMnBr_3$ plotted versus the reduced temperature. The data are taken from reference [25].

6.1. Stacked-triangular antiferromagnets

The best-studied material among the stacked-triangular *XY* antiferromagnets is $CsMnBr_3$, for which specific-heat measurements (exponent α and amplitude ratio A^+/A^-) [26, 27] and neutron scattering measurements (exponents β, γ and ν) [24, 25, 39] were made independently by several groups. The reported values of the exponents and the specific-heat amplitude ratios are summarized in table 4. As an example, the specific-heat data reported in reference [27] and the sublattice-magnetization data reported in reference [25] are reproduced in figures 13 and 14, respectively. All of the authors reported a continuous transition. In particular, high-precision specific-heat measurements gave a stringent upper

limit for the possible latent heat, demonstrating the continuous nature of the transition. Another example of a well-studied $n = 2$ chiral system is $CsNiCl_3$ under high magnetic fields, for which the measured exponents are also included in table 4 [91–93]. Although $CsNiCl_3$ is a weakly Ising-like magnet, under external fields higher than a certain value H_m corresponding to the multicritical point, it exhibits a single transition directly from the paramagnetic state to an 'umbrella-type' non-collinearly ordered state with non-trivial chirality. This is caused because applied fields generate an effective planar anisotropy perpendicular to the field, which cancels and exceeds the intrinsic axial anisotropy. Overall, as can be seen from table 4, the experimental results support the chiral-universality prediction. It should also be noticed that the measured exponents β, γ and ν are not far from the mean-field tricritical values, although the observed ν marginally favours the non-trivial $n = 2$ chiral value. By contrast, the specific-heat exponent α and the amplitude ratio A^+/A^- more or less favour the chiral-universality values over the mean-field tricritical values.

Table 5. Critical exponents and amplitude ratios determined by experiments on several stacked-triangular Heisenberg (or nearly Heisenberg) antiferromagnets. The values given by several theories are also shown. Note that VCl_2, VBr_2 and $RbNiCl_3$ possess weak Ising-like anisotropy, which leads to a small splitting of the transition temperature (35.80 K and 35.88 K in the case of VCl_2; 11.11 K and 11.25 K in the case of $RbNiCl_3$). Since the fully isotropic critical behaviour should be interrupted due to the anisotropy sufficiently close to T_N, one should note that the reported exponents may be affected somewhat by the crossover effect.

	α	β	γ	ν	A^+/A^-
VCl_2	—	0.20(2) [29]	1.05(3) [29]	0.62(5) [29]	—
VBr_2	0.30(5) [30] 0.59(5) and 0.28(2) [28]	—	—	—	0.60(5) [30]
$RbNiCl_3$	0.06(4) [96]	0.25–0.30 [94] 0.27(1) and 0.28(1) [95]	—	—	—
$CsNiCl_3$ at $H = H_m$	0.25(8) [91] 0.23(4) [92]	0.28(3) [93]	—	—	0.52(10) [91]
$CsNiCl_3$ at $H = H_m$	0.28(6) [138]	—	—	—	0.42(10) [92]
Heisenberg	−0.116	0.36	1.387	0.705	1.36
$n = 3$ chiral [21]	0.24(8)	0.30(2)	1.17(7)	0.59(2)	0.54(20)
O(4)	−0.22	0.39	1.47	0.74	—
Mean-field tricritical	0.5	0.25	1	0.5	0

Relatively well-studied Heisenberg-like stacked-triangular antiferromagnets include VCl_2 [29], VBr_2 [28, 30], $RbNiCl_3$ [94–96] as well as $CsNiCl_3$ in an external field corresponding to the multicritical point ($H = H_m$) [91–93]. Note that the former three compounds are nearly Heisenberg systems, possessing a weak axial magnetic anisotropy. The measured values of the exponents and the specific-heat amplitude ratios are summarized in table 5. Except for a relatively large deviation observed in the exponents β and γ for

VCl_2, the results are consistent with $n = 3$ chiral values. Since the high-precision specific-heat measurement for VBr_2 yielded results in good agreement with the theoretical $n = 3$ chiral values, it might be interesting to examine the critical properties of VBr_2 by means of neutron scattering to measure β, γ and ν.

Other stacked-triangular *XY* antiferromagnets that have been studied include $RbMnBr_3$ and $CsCuCl_3$. Unlike those of the compounds quoted above, the lattice structures of these compounds around T_c are distorted from the perfect simple hexagonal lattice. $RbMnBr_3$ exhibits an incommensurate spin order with its turn angle equal to 128° [97], presumably due to its distorted lattice structure [45, 46]. Concerning the critical properties associated with the incommensurate spin order of $RbMnBr_3$, a theoretical argument was given that the critical behaviour will be the same chiral one as for undistorted $CsMnBr_3$ if the lattice deformation of $RbMnBr_3$ is of a certain type [45]. Indeed, for $RbMnBr_3$, Kato *et al* gave $\alpha = 0.42 \pm 0.16$, $\alpha' = 0.22 \pm 0.06$ and $A^+/A^- = 0.30 \pm 0.02$ from birefringence measurements [98], and $\beta = 0.28 \pm 0.02$ from neutron diffraction measurements [99], in reasonable agreement with the expected $n = 2$ chiral values.

By contrast, the lattice structure of $CsCuCl_3$ is distorted such that the anisotropic Dzyaloshinski–Moriya interaction $-\boldsymbol{D}_{ij} \cdot \boldsymbol{S}_i \times \boldsymbol{S}_j$ arises between the neighbouring spins along the *c*-axis, the associated *D*-vector pointing in directions slightly off the *c*-axis (reference [100]). Along the *c*-axis, the directions of these *D*-vectors rotate around the *c*-axis with the period of six lattice spacings. If the *D*-vector were precisely parallel with the *c*-axis, the spin symmetry would be chiral, i.e. $O(2) = Z_2 \times SO(2)$, where Z_2 relates to the chiral degeneracy associated with the non-collinear spin structure *in the triangular layer*. However, the canting of the *D*-vector from the *c*-axis reduces the spin symmetry from the perfect chiral one to a lower one, i.e., only Z_2 associated with the spin inversion. Thus, a crossover from the $n = 2$ chiral critical behaviour is expected in its magnetic transition in the immediate vicinity of T_c [44]. In that sense, $CsCuCl_3$ is not an ideal material for studying the chiral criticality.

The magnetic phase transition of $CsCuCl_3$ was recently studied by means of neutron diffraction by Mekata *et al* [101] and by Schotte *et al* [102], and by specific-heat measurements by Weber *et al* [103]. Mekata *et al* obtained $\beta = 0.25 \pm 0.01$ while Schotte *et al* [102] obtained $\beta = 0.23 \pm 0.02$; these values are close to the $n = 2$ chiral value and that for $CsMnBr_3$. By contrast, Weber *et al* observed over the temperature range $10^{-3} < |t| < 5 \times 10^{-2}$ a power-law scaling behaviour in the specific heat characterized by $\alpha = 0.35 \pm 0.05$ and $A^+/A^- = 0.29 \pm 0.05$, close to the $n = 2$ chiral values, but observed a deviation from this scaling behaviour nearer to T_c. This deviation was interpreted by these authors as a sign of a first-order transition. It was further suggested that this might indicate the failure of chiral universality. It should be noticed, however, that, due to the reduction of spin symmetry caused by the canting of its *D*-vector from the *c*-axis, $CsCuCl_3$ is not an ideal material for studying the $n = 2$ chiral criticality, and the observed deviation from the $n = 2$ chiral critical behaviour might possibly be caused by the expected crossover effect, not being an intrinsic property of an ideal $n = 2$ chiral magnet. The experimental observation reported in reference [103] that external fields applied along the *c*-axis made the deviation from the ideal chiral critical behaviour less pronounced can naturally be understood on the basis of such a crossover picture, because the *c*-axis field tends to confine the non-collinear spin structure in a plane orthogonal to the field, thus relatively weakening the crossover due to the canting effect of the *D*-vector.

One should also note that, as emphasized in section 4.3, theory leaves enough room for the occurrence of a first-order transition even when there exists a chiral universality class. Hence, observation of first-order transition in a few non-collinear magnets is not

quite enough to rule out the possible existence of a chiral universality class for generic non-collinear transitions.

6.2. Helimagnets

In this subsection, I wish to review the experimental situation for helimagnets (spiral magnets). So far, experimental studies of the critical properties of helimagnets have been limited almost exclusively to the rare-earth helimagnets Ho, Dy and Tb. As mentioned in the introduction, the experimental situation for these rare-earth helimagnets has remained confused. Different authors reported considerably different values for the same exponent of the same material, and the reason for this discrepancy has not become clear. Here, I do not intend to give a comprehensive review of various experimental investigations, but rather highlight several points of the most severe conflict, discuss its possible origin and propose possible ways to disentangle the present confusion. For a detailed review of the experimental work on rare-earth helimagnets, I refer the reader to reference [16].

Let us begin with a survey of the present experimental status. Most authors reported that the paramagnetic–helimagnetic transition of Ho, Dy and Tb was continuous.

6.2.1. The exponent α and the specific-heat amplitude ratio A^+/A^-. Several high-precision specific-heat measurements have been made on Ho, Dy and Tb. For Dy, Lederman and Salamon reported a crossover from behaviour characterized by $\alpha = -0.02 \pm 0.01$ and $A^+/A^- = 0.48 \pm 0.02$ ($10^{-2.3} < t < 10^{-0.5}$) to behaviour characterized by $\alpha = 0.18 \pm 0.08$ and $A^+/A^- = 0.44 \pm 0.04$ ($10^{-3.3} < t < 10^{-2.3}$) [7]. Jayasuriya and co-workers gave $\alpha = 0.27 \pm 0.02$ and $A^+/A^- = 1.78 \pm 0.45$ for Ho (reference [104]), $\alpha = 0.24 \pm 0.02$ and $A^+/A^- = 0.41 \pm 0.05$ for Dy (reference [105]), and $\alpha = 0.20 \pm 0.03$ and $A^+/A^- = 0.58 \pm 0.34$ for Tb (reference [106]). Jayasuriya *et al* noticed that the values of α and A^+/A^- changed somewhat according to the form of the fitting formula and the temperature range used in the fit. For Ho, Wang, Belanger and Gaulin gave $\alpha = 0.10 \pm 0.02$ and $A^+/A^- = 0.51 \pm 0.06$ ($0.002 < t < 0.1$), or $\alpha = 0.22 \pm 0.02$ and $A^+/A^- = 0.61 \pm 0.07$ ($0.002 < t < 0.1$), depending on the particular form of the fitting formula [26]. They also reported that the observed critical behaviour could not be well fitted with a single exponent. All of the measurements quoted above agreed in that they all indicate that the transition is continuous. Although there exists considerable scatter among the reported values of α and A^+/A^-, a tendency appears clear: the exponent α tends to be larger than the standard O(n) values and there is a crossover-like behaviour which hinders the data from lying on a single power-law curve in the temperature range studied.

There were also several attempts to extract the specific-heat exponent from some other physical quantities such as electrical resistivity (reference [107]). Since the validity of such procedures was questioned by some authors (reference [105]), I quote here only the results of direct specific-heat measurements.

6.2.2. The exponent β. The exponent β has been measured by neutron, x-ray and Mössbauer techniques. While all of the authors agreed that the transition was continuous, the reported values of β were scattered wildly: 0.21 (Tb; x-ray), 0.23 (Tb; neutron), 0.25 (Tb; neutron), 0.3 (Ho; neutron), 0.335 (Dy; Mössbauer), 0.37 (Ho; x-ray), 0.38 (Dy; neutron), 0.39 (Ho; neutron) to 0.39 (Dy; neutron). It is not easy to read off a systematic tendency from this. Some of the values, particularly that of β for Tb, were close to the $n = 2$ chiral value, but other values, especially those obtained by means of neutron and x-ray diffraction for Ho and Dy, tend to give much larger values close to the O(4) value.

6.2.3. The exponents γ and ν. The exponents γ and ν have been measured by means of neutron and x-ray scattering. Neutron scattering measurements by Gaulin, Hagen and Child gave $\gamma = 1.14 \pm 0.04$ $\nu = 0.57 \pm 0.04$ for Ho, and $\gamma = 1.05 \pm 0.07$, $\nu = 0.57 \pm 0.05$ for Dy, which were close to the $n = 2$ chiral values (reference [108]). More recent x-ray and high-precision neutron scattering studies on Ho by Thurston and co-workers revealed interesting new features (reference [109]). The critical scattering above T_N actually consisted of two components characterized by mutually different exponents: a broad component characterized by the exponents $\nu = 0.55 \pm 0.04$ and $\gamma = 1.24 \pm 0.15$, which was associated with the bulk contribution inside the sample, and a narrow component characterized by the exponents $\nu = 1.0 \pm 0.3$ and $\gamma = 3.4$–4.5, which came from the skin part of the sample. High-precision neutron scattering for Tb also established the existence of two such length scales (reference [110]). Exponents associated with the broad component were in agreement with the earlier measurements. Exponents associated with the narrow component were explained by Altarelli *et al* [111] as governed by the long-range-disorder fixed point (reference [112]), on the assumption that the skin layer of Ho contains a number of edge-dislocation dipoles. Anyway, these experiments have clearly shown that, in order to get the bulk critical properties from the measurements sensitive to the defect-containing skin layer, special care has to be taken to extract the bulk component from the signal.

6.2.4. First-order transition? As already mentioned, a few authors claimed that their experimental data for Ho and Dy were suggestive of a weak first-order transition [11, 12]. Probably, the first experimental claim that the transition in Ho might be weakly first order was made by Tindall, Steinitz and Plumer on the basis of their measurements of the thermal expansion for Ho along the a-axis [11]. These authors observed a jump-like anomaly in the thermal expansivity along the a-axis, although no such anomaly was detected along the c-axis. Tindall *et al* interpreted this anomaly as evidence of a first-order transition. Later measurements by White of the thermal expansion for Ho along the a-axis, however, led to the opposite conclusion that the transition was continuous (reference [113]), and the situation remains unclear. Putting aside such a discrepancy among independent measurements, an apparent jump-like behaviour observed by Tindall *et al* appears to be explained by the standard power-law singularity characteristic of a continuous transition, of the form

$$\Delta a/a \approx b_0 + b_1 t + c_\pm |t|^{1-\tilde{\alpha}} \qquad t \equiv (T - T_N)/T_N$$

if $b_0 > 0$, $b_1 > 0$, $c_+ < 0$ *and* $c_- > 0$, as long as the exponent $\tilde{\alpha}$, usually identified as the specific-heat exponent α, is positive. Note that the coefficients $c_\pm$ could be negative even if the total thermal expansivity is to be positive. Hence, the data of reference [11] cannot be regarded as unequivocal proof of a first-order transition.

While earlier thermal-expansion measurements on the rare-earth metals Dy and Tb indicated a continuous transition (reference [114]), Zachowski *et al* suggested that the paramagnetic–helimagnetic transition of Dy might also be first order on the basis of their observation of deviation from a single power-law scaling behaviour in the immediate vicinity of T_N [12]. Care has to be taken in this interpretation, however, since apparent deviation from the scaling behaviour in a vicinity of T_N could arise from many secondary effects, such as rounding due to impurities or inhomogeneities, insufficiency of temperature control, crossover of an as yet unidentified nature, or even the contribution from the defect-containing skin layer, etc. Therefore, in order to experimentally conclude

that the transition is really first order, one should give a reliable lower bound to the discontinuity of some physical quantity at the transition, such as finite latent heat. At present, there appears to be no such firm experimental evidence of a first-order transition.

6.2.5. Discussion. As shown above, experimental data for rare-earth metals are sometimes mutually conflicting. Below, I wish to try to discuss the possible cause of the conflict together with its possible resolution.

One point to be remembered is that the magnetic interaction in these rare-earth metals is the long-range RKKY interaction whose range is of the order of the pitch of the helix. This means that, when one is far away from T_N and the correlation length is smaller than the helix pitch, one should obtain ordinary mean-field critical behaviour characterized by $\alpha = 0$, $\beta = 0.5$ and $\gamma = 1$ etc [26]. Only when one further approaches T_N and the correlation length gets longer should one obtain a true asymptotic critical behaviour. If one assumes that the asymptotic critical behaviour is also of $n = 2$ chiral universality, one expects a mean-field–$n = 2$ chiral crossover, $\alpha = 0 \rightarrow 0.34$, $\beta = 0.5 \rightarrow 0.25$, $\gamma = 1 \rightarrow 1.13$ etc. In fact, this scenario appears to account for many of the experimental results. For example, earlier specific-heat measurements by Lederman and Salamon [7], where the data exhibited a crossover from a smaller α-value to a larger α-value, appear consistent with this scenario. In the case of γ, since the mean-field value $\gamma = 1$ and the $n = 2$ chiral value $\gamma \simeq 1.13$ happen to be rather close, this crossover would be hard to detect clearly, which is also consistent with experiment (reference [108]).

Another important ingredient might be the possible contribution from the defect-containing skin part of the sample as discussed above. While the contribution from the skin part can be separated above T_N by analysing the line-shape of the scattering function [109, 110], such separation is not straightforward below T_N since the bulk and the skin contributions both yield resolution-limited Bragg peaks. This means that the Bragg intensity observed so far is likely to be a superposition of these two distinct components, each with different exponents β. If one assumes the above scenario, the bulk component exhibits a crossover from $\beta = 0.5$ (ordinary mean-field) to $\beta \simeq 0.25$ ($n = 2$ chiral), while, according to reference [111], the skin component exhibits a behaviour governed by the long-range-disorder fixed point characterized by $\beta = 0.5$. So, a rather complicated situation might indeed occur in rare-earth metals, and special care has to be taken in extracting information about the asymptotic bulk critical behaviour. To my knowledge, experimental analysis fully taking account of such complication has not yet been done especially below T_N. Thus, it is highly desirable to extract the bulk component *below* T_N by separating the contribution of the skin component by some experimental device.

One possible experiment to bypass the above complications might be to study *insulating* helimagnets. There is at least one candidate material, VF_2, which is known to exhibit a paramagnetic–helimagnetic transition (reference [115]). Since the magnetic interaction in VF_2 is *short ranged*, one need not worry about the slow crossover from the mean-field behaviour, and, one hopes, the effect of the defect-containing skin part would be less severe. If so, information about the critical properties of VF_2 would be valuable for disentangling the present complicated situation concerning helimagnets, and I wish to urge experimentalists to try such experiments.

So, one plausible scenario proposed here is that the asymptotic criticality of helimagnets is also of $n = 2$ chiral universality as in the case of stacked-triangular antiferromagnets, which is blurred and masked by the slow crossover from the ordinary mean-field behaviour

caused by the long-range RKKY interaction as well as by the contribution of the defect-containing skin part of the sample. Of course, this hypothesis should be tested by experiments, some of which have been proposed above.

6.3. Measurements of chirality

Chirality is a quantity playing an important role in non-collinear transitions. Hence, it is of great interest to measure the chirality experimentally. Since the chirality is a multispin variable of higher order in the original spin variables, its direct experimental detection needs some ingenuity. Plumer, Kawamura and Caillé pointed out that, if one could prepare a sample with a single chiral domain, the average total chirality $\bar{\kappa}$ could be measured by using polarized neutrons (reference [116]). These authors also suggested that a single chiral domain might be prepared by cooling the sample under applied electric fields. An experimental attempt along these lines was made by Visser *et al* [117]. Maleyev suggested that the chirality might be observable by measuring the polarization-dependent part of the neutron scattering in applied magnetic fields (reference [118]). Fedorov *et al* suggested that the chirality sense might be controlled by applying elastic torsion, which could be used to prepare a single-chiral-domain sample (reference [119]). To the author's knowledge, however, these methods and ideas have not yet been fully substantiated. Direct experimental detection of chirality is certainly a challenging problem, which may serve to provide a new experimental tool for looking into non-collinear ordering.

7. Critical and multicritical behaviours under magnetic fields

In this section, I will review the phase transition of stacked-triangular antiferromagnets under applied magnetic fields. Let us first begin with the case of unfrustrated collinear antiferromagnets on bipartite lattices. Typical magnetic field–temperature phase diagrams of such weakly anisotropic antiferromagnets are illustrated in figure 15 for the cases of axial (Ising-like) anisotropy with the field applied along an easy axis (a), and for the case of planar (XY-like) anisotropy with the field applied in an easy plane (b). Axial magnets in a field exhibit a multicritical point, termed a bicritical point, at which two critical lines and a first-order spin-flop line meet; see figure 15(a). The critical properties of these axial magnets along the critical lines and at the bicritical point were theoretically studied by Fisher and Nelson [120], and by Kosterlitz, Nelson and Fisher [121], with the results given in figure 15. The criticalities are of standard O(n) universality with $n = 1, 2, 3$. Applying a scaling theory, Fisher *et al* derived various predictions, which were supported by subsequent experiments (reference [122]). It thus appears that the critical and the multicritical behaviours of unfrustrated collinear antiferromagnets in a field are now fairly well understood.

For the case of frustrated non-collinear antiferromagnets such as stacked-triangular antiferromagnets, typical magnetic phase diagrams are shown in figure 16 for the cases of axial (Ising-like) anisotropy with the field applied along an easy axis (a), and for the case of planar (XY-like) anisotropy with the field applied in an easy plane (b). In the axial case, three critical lines and a first-order spin-flop line meet at a new type of multicritical point at (T_m, H_m); see figure 16(a). In the planar case, two distinct critical lines meet at a zero-field multicritical point, termed a tetracritical point; see figure 16(b).

Such novel features of the phase diagrams and the multicritical behaviours of stacked-triangular antiferromagnets were first observed experimentally. In the axial case, a phase diagram with a novel multicritical point was found by Johnson, Rayne and Friedberg in

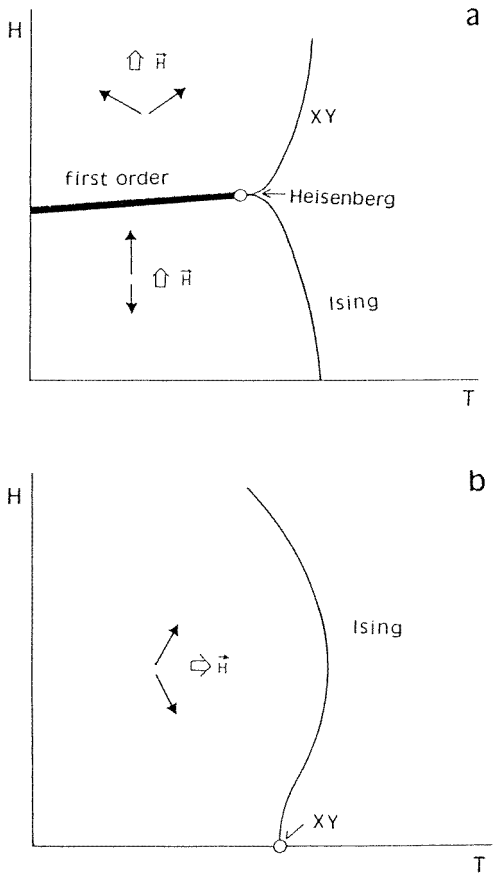

Figure 15. A schematic magnetic field (H) versus temperature (T) phase diagram for a weakly anisotropic unfrustrated antiferromagnet on a bipartite lattice; (a) an axial magnet in a field applied along an easy axis; (b) a planar magnet in a field applied in an easy plane.

1979 for $CsNiCl_3$ by means of susceptibility measurements [38], while in the planar case, a phase diagram with a zero-field tetracritical point was determined by Gaulin *et al* in 1989 for $CsMnBr_3$ by means of neutron scattering measurements [39]. Subsequent phenomenological free-energy analysis successfully reproduced the main qualitative features of these phase diagrams [123, 124]. These multicritical behaviours in a field were also reproduced by subsequent Monte Carlo simulations [125–127].

Scaling analysis of the critical and the multicritical properties of stacked-triangular antiferromagnets under magnetic fields was carried out by Kawamura, Caillé and Plumer on the basis of the chiral-universality scenario [40, 79]: according to this scaling theory, in the axial case, the criticality along the two low-field critical lines is of standard XY universality, while the one along the high-field critical line is of $n = 2$ chiral universality. Meanwhile, the multicritical behaviour right at the multicritical point is predicted to be of $n = 3$ chiral universality. In the planar case, the criticality along the higher-temperature critical line is of XY universality, while that along the lower-temperature critical line is of Ising universality. The multicritical (tetracritical) behaviour at the zero-field transition point is of $n = 2$ chiral universality governed by the $n = 2$ chiral fixed point.

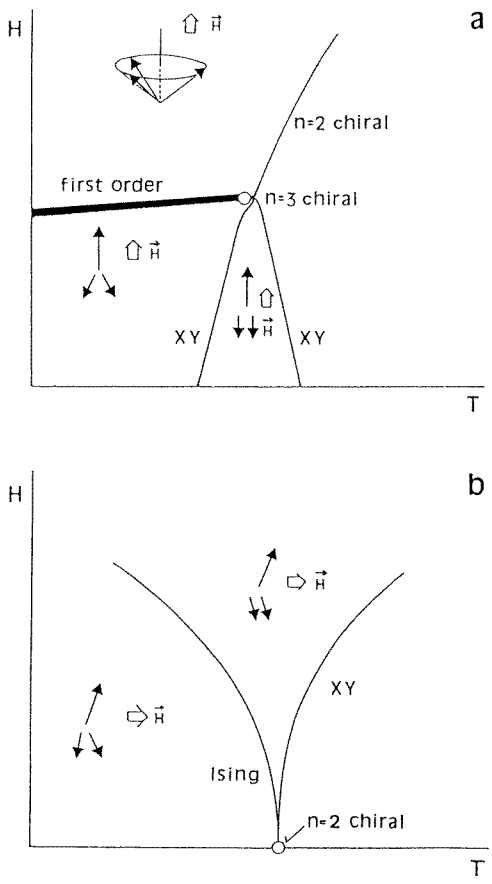

Figure 16. A schematic magnetic field (H) versus temperature (T) phase diagram of a weakly anisotropic frustrated antiferromagnet on a stacked-triangular lattice; (a) an axial magnet in a field applied along an easy axis; (b) a planar magnet in a field applied in an easy plane.

Scaling theory further predicted that, in the axial case, three critical lines should merge at the multicritical point tangentially with the first-order spin-flop line as [40]

$$|H - H_m| \propto |T - T_m|^{\phi} \tag{7.1}$$

where the exponent $\phi \sim 1.06$ is common among the three critical lines. In fact, ϕ is the anisotropy-crossover exponent at the $n = 3$ chiral fixed point identified in the RG analysis in section 4.2.

Similarly, in the planar case, it is predicted that the two critical lines in external fields should merge at the zero-field tetracritical point as [40]

$$H^2 \propto |T - T_m|^{\phi} \tag{7.2}$$

where $\phi \sim 1.04$ is the anisotropy-crossover exponent at the $n = 2$ chiral fixed point, common between the two critical lines. Near the tetracritical point, the zero-field uniform susceptibility was predicted to behave as [40, 42, 79]

$$\chi(T, H = 0) \approx C_{\pm}|T - T_m|^{-\tilde{\gamma}} + \text{less singular and regular parts} \tag{7.3}$$

where $\tilde{\gamma} = -(2 - \alpha - \phi) \sim -0.56$.

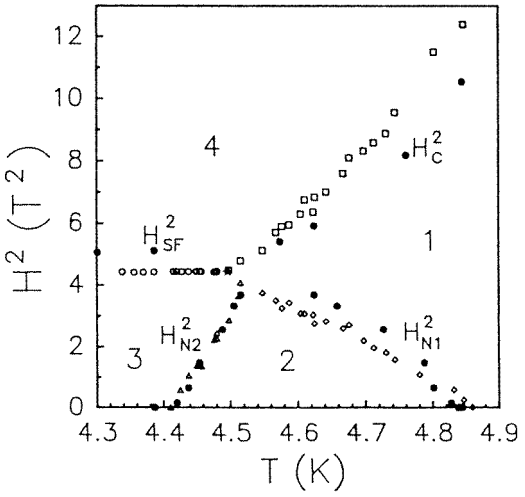

Figure 17. The magnetic phase diagram of the axial stacked-triangular antiferromagnet $CsNiCl_3$ near the multicritical point as determined by sound-velocity measurements. The regions labelled 1–4 refer to the four phases in figure 16(a). The data are taken from reference [128].

These scaling predictions were tested by subsequent experiments. In the axial case, criticality along the three critical lines as well as at the multicritical point were examined by several authors. In particular, the predicted $n = 2$ chiral behaviour along the high-field critical line as well as the $n = 3$ chiral behaviour at the multicritical point were very well confirmed by specific-heat measurements by Beckmann, Wosnitza and von Löhneysen on $CsNiCl_3$ [91], by birefringence measurements by Enderle, Furtuna and Steiner on $CsNiCl_3$ and $CsMnI_3$ [92] and by neutron diffraction measurements by Enderle, Schneider, Matsuoka and Kakurai on $CsNiCl_3$ [93]. The behaviour of the phase boundaries near the multicritical point was investigated by Poirier *et al* for $CsNiCl_3$, who found by means of ultrasonic velocity measurements that the low-temperature low-field critical line between the collinear and non-collinear phases (regions 2 and 3 in figure 17) exhibited a 'turnover' in the immediate vicinity of the multicritical point to merge into the first-order spin-flop line, as shown in figure 17 (reference [128]). This turnover behaviour was not expected from the mean-field theory, but was in accord with the scaling prediction. Katori, Goto and Ajiro [129] and Asano *et al* [130] determined by magnetization measurements the phase diagrams of other axial stacked-triangular antiferromagnets, $CsNiBr_3$ and $CsMnI_3$, and emphasized universal aspects of the phase diagrams.

Along the two low-field critical lines, theory predicts the standard *XY* critical behaviour. Experimentally, the critical properties at these two transition points were studied in zero field by several methods, including those of NMR (reference [131]), neutron scattering (reference [132]) for $CsNiCl_3$, and neutron scattering (references [133, 134]) and specific heat (reference [135]) for $CsMnI_3$. Most of the results are consistent with the expected *XY* criticality, although significant deviation was observed in a few cases, such as the exponents γ and ν reported in reference [134]. Some of such deviation may be ascribed to the proximity effect of the $n = 3$ chiral behaviour realized at the multicritical point at $H = H_m$.

In the planar case, the situation is not entirely satisfactory. As regards the behaviour of the two critical lines near the zero-field tetracritical point, Gaulin *et al* reported, on the basis

of neutron scattering for $CsMnBr_3$, the crossover exponents $\phi_{P-II} \sim 1.21$ and $\phi_{II-I} \sim 0.75$ for the high- and low-temperature critical lines, respectively, which differed considerably from the scaling results, $\phi_{P-II} = \phi_{II-I} \sim 1$. Reanalysis of the data given by Gaulin *et al*, however, revealed that, once the uncertainty of T_m was taken into account in the analysis, the experimental data were not inconsistent with the scaling results [42]. Goto, Inami and Ajiro found from magnetization measurements $\phi_{P-II} = 1.02 \pm 0.05$ and $\phi_{II-I} = 1.07 \pm 0.05$ for $CsMnBr_3$ (reference [136]); these values were in good agreement with the theoretical values. By contrast, markedly smaller values, $\phi_{P-II} = 0.78 \pm 0.06$ and $\phi_{II-I} = 0.79 \pm 0.06$, were reported by Tanaka, Nakano and Matsuo for the *XY* stacked-triangular antiferromagnet $CsVBr_3$, on the basis of susceptibility measurements (reference [137]), while the values $\phi_{P-II} = 0.76 \pm 0.1$ and $\phi_{II-I} = 0.81 \pm 0.1$ were reported by Weber, Beckmann, Wosnitza and von Löhneysen for $CsMnBr_3$, on the basis of specific-heat measurements (reference [138]). The cause of this discrepancy is not clear. From the theoretical side, although the prediction that the exponent ϕ is common among the critical lines is a direct consequence of the chiral-universality picture, its precise value is still subject to large uncertainties, because it has not yet been determined by reliable numerical methods such as extensive Monte Carlo simulation. It is thus desirable to give a more reliable numerical estimate of the anisotropy-crossover exponent ϕ.

It turns out that the zero-field transition point of $RbMnBr_3$ is also a tetracritical point in the magnetic field–temperature phase diagram [139–141]. The associated crossover exponents were determined by Heller *et al* by means of neutron scattering as 1.00 ± 0.35 and 1.07 ± 0.25, for the higher-temperature and the lower-temperature critical lines, respectively (reference [141]).

The zero-field susceptibility of $CsMnBr_3$ was measured by Mason, Stager, Gaulin and Collins [142]. These authors interpreted their data as being inconsistent with the scaling prediction on the assumption that the coefficients of the leading singularity, $C_\pm$ in equation (7.3), were both positive and that the contribution from the regular and less singular terms was zero. However, once one properly takes account of the fact that the sign of $C_\pm$ could be different on either side of T_m and that there is generally a finite contribution from the regular and less singular terms, the experimental data are consistent with the scaling theory [42, 79].

8. Summary

Recent theoretical and experimental studies on phase transitions of non-collinear or canted magnets, including both stacked-triangular antiferromagnets and helimagnets, were reviewed with particular emphasis on the novel critical and multicritical behaviours observed for these magnets.

Theoretical analyses based on various renormalization-group techniques, which usually gave good results for standard unfrustrated magnets, have given somewhat inconclusive and sometimes conflicting results concerning the nature of the non-collinear transitions. Special care appears to be necessary in applying the standard RG methods to a system with non-trivial structure in the order-parameter space as in the present problem. Nevertheless, as was discussed in detail in section 4, a most plausible possibility suggested on the basis of the RG analyses is that either the transition is continuous, governed by a new fixed point (chiral universality), or the transition is first order.

Most of the recent extensive Monte Carlo simulations performed on *XY* and Heisenberg stacked-triangular antiferromagnets suggest the occurrence of a continuous transition characterized by exponents significantly different from the standard $O(n)$ exponents. In that

sense, these Monte Carlo results support the chiral-universality scenario. The bulk of various experiments on stacked-triangular *XY* and Heisenberg antiferromagnets have also yielded results in favour of the chiral-universality scenario: a continuous transition characterized by novel exponents close to those obtained by Monte Carlo simulations has been observed. Meanwhile, in the case of *XY* spins, many of the Monte Carlo and experimental results also appear to be marginally consistent with mean-field tricritical behaviour, while such behaviour is not suggested by some of the data such as the specific-heat exponents, specific-heat amplitude ratios and chirality exponents. From a theoretical viewpoint, the mean-field tricritical behaviour dictated by the trivial Gaussian fixed point is rather unlikely even when the system happens to be just at its tricriticality, as long as the generic non-collinear criticality is *not* of the standard O(n) universality. Thus, at least in the case of stacked-triangular antiferromagnets, there appears to be reasonable evidence both from Monte Carlo simulations and experiments that a new chiral universality class is in fact realized.

There still seems to exist a slight chance of a weak first-order transition, though, indicated by either Monte Carlo simulations or experiments. Although this point needs to be examined, it seems already clear from recent extensive studies that there exists a rather wide and well-defined critical region, say $10^{-1} > t > 10^{-3}$, characterized by a set of novel critical exponents and amplitude ratios, *which are universal for various non-collinear magnetic materials and model systems*. This observation strongly suggests *the existence of an underlying novel fixed point governing the non-collinear criticality*. The remaining possibility is that this fixed point may be slightly complex valued. It is certainly interesting to examine further the order of the transition both via careful numerical simulations and via high-precision experiments, either to get unambiguous evidence of a first-order transition or to push the limit of the continuous nature of the transition further. To do this experimentally, one needs to choose appropriate materials which do not have a weak perturbative interaction which breaks the chiral symmetry. In addition, to be sure that the transition is first order, one should give a reliable lower bound on the discontinuity of some physical quantities such as the latent heat. Mere observation of deviation from a simple power-law behaviour in the immediate vicinity of T_N is not quite enough to allow one to conclude that the transition is first order, since such deviation could arise from many secondary effects. Also, one should recognize that, even when there exists a well-defined chiral universality class, it is entirely possible that some systems sharing the same chiral symmetry exhibit first-order transitions due to the difference in non-universal details of certain microscopic parameters.

Compared to the case for stacked-triangular antiferromagnets, the present situation for helimagnets (spiral magnets) is less clear. In particular, the experimental situation for rare-earth helimagnets has been confused for years now. I have proposed one possible scenario for resolving this confusion based on the chiral-universality scenario, where the combined effects of the long-range nature of the RKKY interaction and the contribution from the defect-containing skin part hinder the observation of an ideal chiral critical behaviour. It might be interesting to test the proposal by carrying out further experiments. On the numerical side, it might be interesting to perform further Monte Carlo simulations on helimagnets, paying attention to the effects of boundary conditions.

To sum up, the phase transitions of frustrated non-collinear magnets exhibit novel behaviours different from those exhibited by standard unfrustrated collinear magnets. Although there is not a complete consensus among researchers, many experimental and numerical results on stacked-triangular antiferromagnets point to the occurrence of phase transitions of a new chiral universality class, distinct from the standard O(n) Wilson–Fisher universality class. As a reflection of richer structure of its order parameter, the non-collinear transitions also possess some unique physical quantities such as chirality which have no

counterpart for the standard unfrustrated magnets. Such rich inner symmetry also leads to unique magnetic phase diagrams in external fields with novel multicritical behaviours. In this decade, there has been a stimulating and fruitful interplay between theory and experiment in this area. Hopefully, further theoretical as well as experimental work will clarify novel features of the non-collinear transitions, which might serve to enlarge and deepen our understanding of phase transitions and critical phenomena.

Acknowledgment

The author is grateful to Professor D P Belanger for a reading of the manuscript.

References

[1] Villain J 1977 *J. Phys. C: Solid State Phys.* **10** 4793
[2] Miyashita S and Shiba H 1985 *J. Phys. Soc. Japan* **53** 1145
[3] Kawamura H and Miyashita S 1984 *J. Phys. Soc. Japan* **53** 4138
[4] Bak P and Mukamel D 1976 *Phys. Rev.* B **13** 5086
[5] Garel T and Pfeuty P 1976 *J. Phys. C: Solid State Phys.* **9** L245
[6] Eckert J and Shirane G 1976 *Solid State Commun.* **19** 911
[7] Lederman E L and Salamon M B 1974 *Solid State Commun.* **15** 1373
[8] Loh E, Chien C L and Walker J C 1974 *Phys. Lett.* **49A** 357
[9] Dietrich O W and Als-Nielsen J 1967 *Phys. Rev.* **162** 315
[10] Barak Z and Walker M B 1982 *Phys. Rev.* B **25** 1969
[11] Tindall D A, Steinitz M O and Plumer M L 1977 *J. Phys. F: Met. Phys.* **7** L263
[12] Zachowski S W, Tindall D A, Kahrizi M, Genossar J and Steinitz M O 1986 *J. Magn. Magn. Mater.* **54–57** 707
[13] Tang C C, Stirling W G, Jones D L, Wilson C C, Haycock P W, Rollason A J, Thomas A H and Fort D 1992 *J. Magn. Magn. Mater.* **103** 86
[14] Tang C C, Haycock P W, Stirling W G, Wilson C C, Keen D and Fort D 1995 *Physica* B **205** 105
[15] Thurston T R, Helgesen G, Hill J P, Gibbs D, Gaulin B D and Simpson P J 1994 *Phys. Rev.* B **49** 15 730
[16] du Plessis P de V, Venter A M and Brits G H F 1995 *J. Phys.: Condens. Matter* **7** 9863
[17] du Plessis P de V, van Doorn C F and van Delden D C 1983 *J. Magn. Magn. Mater.* **40** 91
[18] Brits G H F and du Plessis P de V 1988 *J. Phys. F: Met. Phys.* **18** 2659
[19] Kawamura H 1985 *J. Phys. Soc. Japan* **54** 3220
Kawamura H 1987 *J. Phys. Soc. Japan* **56** 474
[20] Kawamura H 1986 *J. Phys. Soc. Japan* **55** 2095
Kawamura H 1989 *J. Phys. Soc. Japan* **58** 584
[21] Kawamura H 1992 *J. Phys. Soc. Japan* **61** 1299
[22] Kawamura H 1988 *J. Appl. Phys.* **63** 3086
[23] Kawamura H 1988 *Phys. Rev.* B **38** 4916 (erratum 1990 **42** 2610)
[24] Mason T E, Collins M F and Gaulin B D 1987 *J. Phys. C: Solid State Phys.* **20** L945
Mason T E, Collins M F and Gaulin B D 1989 *Phys. Rev.* B **39** 586
[25] Ajiro Y, Nakashima T, Unno Y, Kadowaki H, Mekata M and Achiwa N 1988 *J. Phys. Soc. Japan* **57** 2648
Kadowaki H, Shapiro S M, Inami T and Ajiro Y 1988 *J. Phys. Soc. Japan* **57** 2640
[26] Wang J, Belanger D P and Gaulin B D 1991 *Phys. Rev. Lett.* **66** 3195
[27] Deutschmann R, von Löhneysen H, Wosnitza J, Kremer R K and Visser D 1992 *Europhys. Lett.* **17** 637
[28] Takeda K, Uryû N, Ubukoshi K and Hirakawa K 1986 *J. Phys. Soc. Japan* **55** 727
[29] Kadowaki H, Ubukoshi K, Hirakawa K, Martinéz J L and Shirane G 1988 *J. Phys. Soc. Japan* **56** 4027
[30] Wosnitza J, Deutschmann R, von Löhneysen H and Kremer R K 1994 *J. Phys.: Condens. Matter* **6** 8045
[31] Azaria P, Delamotte B and Jolicoeur Th 1990 *Phys. Rev. Lett.* **64** 3175
[32] Azaria P, Delamotte B, Delduc F and Jolicoeur Th 1993 *Nucl. Phys.* B **408** 485
[33] Bhattacharya T, Billoire A, Lacaze R and Jolicoeur Th 1994 *J. Physique* **4** 181
[34] Boubcheur E H, Loison D and Diep H T 1996 *Phys. Rev.* B **54** 4165
[35] Loison D and Diep H T 1994 *Phys. Rev.* B **50** 16 453
[36] Plumer M L and Mailhot A 1994 *Phys. Rev.* B **50** 16 113
[37] Mailhot A, Plumer M L and Caillé A 1994 *Phys. Rev.* B **50** 6854

[38] Johnson P B, Rayne J A and Friedberg S A 1979 *J. Appl. Phys.* **50** 583
[39] Gaulin B D, Mason T E, Collins M F and Larese J Z 1989 *Phys. Rev. Lett.* **62** 1380
[40] Kawamura H, Caillé A and Plumer M L 1990 *Phys. Rev.* B **41** 4416
[41] Kawamura H 1992 *Recent Advances in Magnetism of Transition Metal Compounds* ed A Kotani and N Suzuki (Singapore: World Scientific) p 335
[42] Gaulin B D 1994 *Magnetic Systems with Competing Interactions* ed H T Diep (Singapore: World Scientific) p 286
[43] Plumer M L, Caillé A, Mailhot A and Diep H T 1994 *Magnetic Systems with Competing Interactions* ed H T Diep (Singapore: World Scientific) p 1
[44] Collins M F and Petrenko O A 1997 *Can. J. Phys.* **75** 605
[45] Kawamura H 1990 *Prog. Theor. Phys. Suppl.* **101** 545
[46] Zhang W, Saslow W M and Gabay M 1991 *Phys. Rev.* B **44** 5129
Zhang W, Saslow W M, Gabay M and Benakli M 1993 *Phys. Rev.* B **48** 10 204
[47] Jones D R T, Love A and Moore M A 1976 *J. Phys. C: Solid State Phys.* **9** 743
[48] Bailin D, Love A and Moore M A 1977 *J. Phys. C: Solid State Phys.* **10** 1159
[49] Joynt R 1991 *Europhys. Lett.* **16** 289
Joynt R 1993 *Phys. Rev. Lett.* **71** 3015
[50] Granato E and Kosterlitz J M 1990 *Phys. Rev. Lett.* **65** 1267
[51] Toulouse G and Kléman M 1976 *J. Physique Lett.* **37** 149
Mermin N D 1979 *Rev. Mod. Phys.* **51** 591
[52] Kosterlitz J M and Thouless D J 1973 *J. Phys. C: Solid State Phys.* **6** 1181
Kosterlitz J M 1974 *J. Phys. C: Solid State Phys.* **7** 1046
[53] Lee D H, Joannopoulos J D, Negele J W and Landau D P 1984 *Phys. Rev. Lett.* **52** 433
Lee D H, Joannopoulos J D, Negele J W and Landau D P 1986 *Phys. Rev.* B **33** 450
[54] Teitel S and Jayaprakash C 1983 *Phys. Rev.* B **27** 598
[55] Ramirez-Santiago G and José J V 1992 *Phys. Rev. Lett.* **68** 1224
Ramirez-Santiago G and José J V 1994 *Phys. Rev.* **49** 9567 and references therein
[56] Olsson P 1995 *Phys. Rev. Lett.* **75** 2758 and references therein
[57] Wintel M, Everts H U and Apel W 1995 *Phys. Rev.* B **52** 13 480
[58] Kawamura H and Kikuchi M 1993 *Phys. Rev.* B **47** 1134
[59] Southern B W and Xu H-J 1995 *Phys. Rev.* B **52** R3836
[60] Kohring G, Shrock R E and Wills P 1986 *Phys. Rev. Lett.* **57** 1358
Williams G 1987 *Phys. Rev. Lett.* **59** 1926
Shenoy S R 1989 *Phys. Rev.* B **40** 7212
[61] Antonenko S A, Sokolov A I and Varnashev K B 1995 *Phys. Lett.* **208A** 161
[62] Mudrov A I and Varnashev K B 1997 *Preprint* cond-mat/9712007
Mudrov A I and Varnashev K B 1998 *Preprint* cond-mat/9802064
[63] Antonenko S A and Sokolov A I 1994 *Phys. Rev.* B **49** 15 901
[64] Cowley R A and Bruce A D 1978 *J. Phys. C: Solid State Phys.* **11** 3577
[65] Shpot N A 1989 *Phys. Lett.* **142** 474
[66] Kawamura H, unpublished
[67] Kawamura H 1988 *Phys. Rev.* B **38** 960
[68] Jolicoeur Th 1995 *Europhys. Lett.* **30** 555
[69] Halperin B I, Lubensky T C and Ma S K 1974 *Phys. Rev. Lett.* **32** 292
[70] Dasgupta C and Halperin B I 1981 *Phys. Rev. Lett.* **47** 1556
[71] Olsson P and Teitel S 1997 *Preprint* cond-mat/9710200 and references therein
[72] Radzihovsky L 1995 *Europhys. Lett.* **29** 227
[73] Kleinert H, Thomas S and Schote-Frohline V 1997 *Phys. Rev.* B **56** 14 428 and references therein
[74] Kawamura H, unpublished
[75] Kunz H and Zumbach G 1993 *J. Phys. A: Math. Gen.* **26** 3121
[76] Dobry A and Diep H T 1995 *Phys. Rev.* **51** 6731
[77] Zumbach G 1993 *Phys. Rev. Lett.* **71** 2421
[78] Zumbach G 1994 *Phys. Lett.* **190A** 225
Zumbach G 1994 *Nucl. Phys.* B **413** 771
[79] Kawamura H 1993 *Phys. Rev.* B **47** 3415
[80] Kawamura H 1991 *J. Phys. Soc. Japan* **60** 1839
[81] Zumbach G 1995 *Nucl. Phys.* B **435** 753
[82] David F and Jolicoeur Th 1996 *Phys. Rev. Lett.* **76** 3148

[83] See, for example,
Castilla G E and Chakravarty S 1993 *Phys. Rev. Lett.* **71** 384
Castilla G E and Chakravarty S 1997 *Nucl. Phys.* B **485** 613 and references therein
[84] Kawamura H 1990 *J. Phys. Soc. Japan* **59** 2305
[85] Saul L 1992 *Phys. Rev.* B **46** 13 847
[86] Reimers J N, Greedan J E and Björgvinsson M 1992 *Phys. Rev.* B **45** 7295
[87] Mailhot A and Plumer M L 1993 *Phys. Rev.* B **48** 9881
[88] Plumer M L and Mailhot A 1997 *J. Phys.: Condens. Matter* **9** L165
[89] Diep H T 1989 *Phys. Rev.* B **39** 397
[90] Saslow W M, Gabay M and Zhang W 1992 *Phys. Rev. Lett.* **68** 3627
[91] Beckmann D, Wosnitza J and von Löhneysen H 1993 *Phys. Rev. Lett.* **71** 2829
[92] Enderle M, Furtuna G and Steiner M 1994 *J. Phys.: Condens. Matter* **6** L385
[93] Enderle M, Schneider R, Matsuoka Y and Kakurai K 1997 *Physica* B **234–236** 554
[94] Yelon W B and Cox D E 1972 *Phys. Rev.* B **6** 204
[95] Oohara Y, Kadowaki H and Iio K 1991 *J. Phys. Soc. Japan* **60** 393
[96] Oohara Y, Iio K and Tanaka H 1991 *J. Phys. Soc. Japan* **60** 4280
[97] Eibshütz E, Sherwood R, Hsu F L and Cox D E 1972 *AIP Conf. Proc.* **17** 684
[98] Kato T, Iio K, Hoshino T, Mitsui T and Tanaka H 1992 *J. Phys. Soc. Japan* **61** 275
[99] Kato T, Asano T, Ajiro Y, Kawano S, Ishii T and Iio K 1995 *Physica* B **213+214** 182
[100] Tanaka H, Iio K and Nagata K 1985 *J. Phys. Soc. Japan* **54** 4345
[101] Mekata M, Ajiro Y, Sugino T, Oohara A, Ohara K, Yasuda S, Oohara S and Yoshizawa H 1995 *J. Magn. Magn. Mater.* **140–144** 38
[102] Schotte U, Stüsser N, Schotte K D, Weinfurter H, Mayer H M and Winkelmann M 1994 *J. Phys.: Condens. Matter* **6** 10 105
Stüsser N, Schotte U, Schotte K D and Hu X 1995 *Physica* B **213+214** 164
[103] Weber H B, Werner T, Wosnitza J and von Löhneysen H 1996 *Phys. Rev.* B **54** 15 924
[104] Jayasuriya K D, Campbell S J and Stewart A M 1985 *J. Phys. F: Met. Phys.* **15** 225
[105] Jayasuriya K D, Campbell S J and Stewart A M 1985 *Phys. Rev.* B **31** 6032
[106] Jayasuriya K D, Stewart A M, Campbell S J and Gopal E S R 1984 *J. Phys. F: Met. Phys.* **14** 1725
[107] See, e.g.,
Balberg I and Maman A 1979 *Physica* B **96** 54
[108] Gaulin B D, Hagen M and Child H R 1988 *J. Physique Coll.* **49** 327
[109] Thurston T R, Helgesen G, Gibbs D, Hill J P, Gaulin B D and Shirane G 1993 *Phys. Rev. Lett.* **70** 3151
[110] Gehring P M, Hirota K, Majkrzak C F and Shirane G 1993 *Phys. Rev. Lett.* **71** 1087
Hirota K, Shirane G, Gehring P M and Majkrzak C 1994 *Phys. Rev.* B **49** 11 967
[111] Altarelli M, Núnez-Rugueiro M D and Papoular M 1995 *Phys. Rev. Lett.* **74** 3840
[112] Weinrib A and Halperin B I 1983 *Phys. Rev.* B **27** 413
[113] White G K 1989 *J. Phys. C: Solid State Phys.* **1** 6987
[114] Tindall D A and Steinitz M O 1983 *J. Phys. F: Met. Phys.* **13** L71
[115] Stout J W and Boo W O J 1966 *J. Appl. Phys.* **37** 966
Stout J W and Lau H Y 1967 *J. Appl. Phys.* **38** 1472
Lau H Y, Stout J W, Koehler W C and Child H R 1969 *J. Appl. Phys.* **40** 1136
[116] Plumer M L, Kawamura H and Caillé A 1991 *Phys. Rev.* B **43** 13 786
[117] Visser D, Coldwell T R, McIntyre G J, Graf H, Weiss L, Zeiske Th and Plumer M L 1994 *Ferroelectrics* **162** 147
[118] Maleyev S V 1995 *Phys. Rev. Lett.* **75** 4682
[119] Fedorov V I, Gukasov A G, Kozlov V, Maleyev S V, Plakhty V P and Zobkalo I A 1997 *Phys. Lett.* **224A** 372
[120] Fisher M E and Nelson D R 1974 *Phys. Rev. Lett.* **32** 1350
[121] Kosterlitz J M, Nelson D R and Fisher M E 1976 *Phys. Rev.* B **13** 412
[122] See, for example,
King A R and Rohrer H 1979 *Phys. Rev.* B **19** 5864
[123] Plumer M L, Hood K and Caillé A 1988 *Phys. Rev. Lett.* **60** 45
[124] Plumer M L and Caillé A 1990 *Phys. Rev.* B **41** 2543
[125] Mailhot A, Plumer M L and Caillé A 1993 *Phys. Rev.* B **48** 15 835
[126] Mason T E, Collins M F and Gaulin B D 1990 *J. Appl. Phys.* **67** 5421
[127] Plumer M L and Caillé A 1990 *Phys. Rev.* B **42** 10 388
[128] Poirier M, Caillé A and Plumer M L 1990 *Phys. Rev.* B **41** 4869

[129] Katori H A, Goto T and Ajiro Y 1993 *J. Phys. Soc. Japan* **62** 743
[130] Asano T, Ajiro Y, Mekata M, Aruga Katori H and Goto T 1994 *Physica* B **201** 75
[131] Clark R H and Moulton W G 1972 *Phys. Rev.* B **5** 788
[132] Kadowaki H, Ubukoshi K and Hirakawa K 1987 *J. Phys. Soc. Japan* **56** 751
[133] Ajiro Y, Inami T and Kadowaki H 1990 *J. Phys. Soc. Japan* **59** 4142
[134] Kadowaki H, Inami T, Ajiro Y, Nakajima K and Endoh Y 1991 *J. Phys. Soc. Japan* **56** 1708
[135] Beckmann D, Wosnitza J, von Löhneysen H and Visser D 1993 *J. Phys.: Condens. Matter* **5** 6289
[136] Goto T, Inami T and Ajiro Y 1990 *J. Phys. Soc. Japan* **59** 2328
[137] Tanaka H, Nakano H and Matsuo S 1994 *J. Phys. Soc. Japan* **63** 3169
[138] Weber H, Beckmann D, Wosnitza J and von Löhneysen H 1995 *Int. J. Mod. Phys.* B **9** 1387
[139] Kawano S, Ajiro Y and Inami T 1992 *J. Magn. Magn. Mater.* **104–107** 791
[140] Kato T, Ishii T, Ajiro Y, Asano T and Kawano S 1993 *J. Phys. Soc. Japan* **62** 3384
[141] Heller L, Collins M F, Yang Y S and Collier B 1994 *Phys. Rev.* B **49** 1104
[142] Mason T E, Stager C V, Gaulin B D and Collins M F 1990 *Phys. Rev.* B **42** 2715